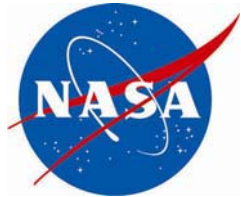


NASA/TM-2008-215338
NESC-RP-08-09/06-081-E



Ares I-X USS Material Testing

*David S. Dawicke
Analytical Services and Materials, Hampton, Virginia*

*Stephen W. Smith
NASA Langley Research Center, Hampton, Virginia*

*Ivatury S. Raju
NASA Langley Research Center, Hampton, Virginia*

The NASA STI Program Office . . . in Profile

Since its founding, NASA has been dedicated to the advancement of aeronautics and space science. The NASA Scientific and Technical Information (STI) Program Office plays a key part in helping NASA maintain this important role.

The NASA STI Program Office is operated by Langley Research Center, the lead center for NASA's scientific and technical information. The NASA STI Program Office provides access to the NASA STI Database, the largest collection of aeronautical and space science STI in the world. The Program Office is also NASA's institutional mechanism for disseminating the results of its research and development activities. These results are published by NASA in the NASA STI Report Series, which includes the following report types:

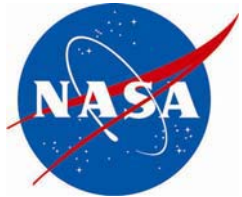
- **TECHNICAL PUBLICATION.** Reports of completed research or a major significant phase of research that present the results of NASA programs and include extensive data or theoretical analysis. Includes compilations of significant scientific and technical data and information deemed to be of continuing reference value. NASA counterpart of peer-reviewed formal professional papers, but having less stringent limitations on manuscript length and extent of graphic presentations.
- **TECHNICAL MEMORANDUM.** Scientific and technical findings that are preliminary or of specialized interest, e.g., quick release reports, working papers, and bibliographies that contain minimal annotation. Does not contain extensive analysis.
- **CONTRACTOR REPORT.** Scientific and technical findings by NASA-sponsored contractors and grantees.
- **CONFERENCE PUBLICATION.** Collected papers from scientific and technical conferences, symposia, seminars, or other meetings sponsored or co-sponsored by NASA.
- **SPECIAL PUBLICATION.** Scientific, technical, or historical information from NASA programs, projects, and missions, often concerned with subjects having substantial public interest.
- **TECHNICAL TRANSLATION.** English-language translations of foreign scientific and technical material pertinent to NASA's mission.

Specialized services that complement the STI Program Office's diverse offerings include creating custom thesauri, building customized databases, organizing and publishing research results ... even providing videos.

For more information about the NASA STI Program Office, see the following:

- Access the NASA STI Program Home Page at <http://www.sti.nasa.gov>
- E-mail your question via the Internet to help@sti.nasa.gov
- Fax your question to the NASA STI Help Desk at (301) 621-0134
- Phone the NASA STI Help Desk at (301) 621-0390
- Write to:
NASA STI Help Desk
NASA Center for AeroSpace Information
7115 Standard Drive
Hanover, MD 21076-1320

NASA/TM-2008-215338
NESC-RP-08-09/06-081-E



Ares I-X USS Material Testing

David S. Dawicke
Analytical Services and Materials, Hampton, Virginia

Stephen W. Smith
NASA Langley Research Center, Hampton, Virginia

Ivatury S. Raju
NASA Langley Research Center, Hampton, Virginia

NASA Engineering and Safety Center
Langley Research Center
Hampton, Virginia 23681-2199

August 2008

The use of trademarks or names of manufacturers in the report is for accurate reporting and does not constitute an official endorsement, either expressed or implied, of such products or manufacturers by the National Aeronautics and Space Administration.

Available from:
NASA Center for AeroSpace Information (CASI)
7115 Standard Drive
Hanover, MD 21076-1320
(301) 621-0390

Abstract

An independent assessment was conducted to determine the critical initial flaw size (CIFS) for the flange-to-skin weld in the Ares I-X Upper Stage Simulator (USS). Material characterization tests were conducted to quantify the material behavior for use in the CIFS analyses. Fatigue crack growth rate, Charpy impact, and fracture tests were conducted on the parent and welded A516 Grade 70 steel. The crack growth rate tests confirmed that the material behaved in agreement with literature data and that a salt water environment would not significantly degrade the fatigue resistance. The Charpy impact tests confirmed that the fracture resistance of the material did not have a significant reduction for the expected operational temperatures of the vehicle. Finally, the fracture toughness tests resulted in a lower bound fracture toughness (K_c) value of 65 ksi inch^{1/2}.

Introduction

An independent assessment was conducted to determine the critical initial flaw size (CIFS) for the flange-to-skin weld in the Ares I-X Upper Stage Simulator (USS). The skin and flange are made of A516 Grade 70 steel and the flange-to-skin weld was initially performed using a pulse MIG process, but the process was changed to a flux-cored welding process for the final production of the USS. Tests were conducted to evaluate the material behavior of the A516 steel with particular attention to the material behavior that could be influenced by the weld process. The types of tests that were run include: fatigue crack growth rate in lab air and in a salt-water environment, Charpy impact tests, and fracture tests. Parent A516 material was used for the fatigue crack growth rate tests and plates of welded material were used for the Charpy impact (flux-cored process) and fracture (both flux cored and pulse MIG processes) tests.

The welded plates for testing were created by both a flux-core and a pulse MIG welding process that joined a $\frac{1}{2}$ inch thick plate to a 1-inch thick plate. The 1-inch thick plate was intended to simulate the flange and the $\frac{1}{2}$ inch thick plate simulated the skin. Unlike the actual structure, the flange was rotated 90 degrees to allow sufficient material for manufacture of the specimens, as shown in Figure 1. After welding, the flange material was machined to a thickness of $\frac{1}{2}$ inch to allow for testing with standard specimen configurations. The weld consisted of a single bevel on the skin side and was straight on the flange side, as illustrated in the edge etch shown in Figure 2. The following sections describe the tests conducted on the parent and weld materials.

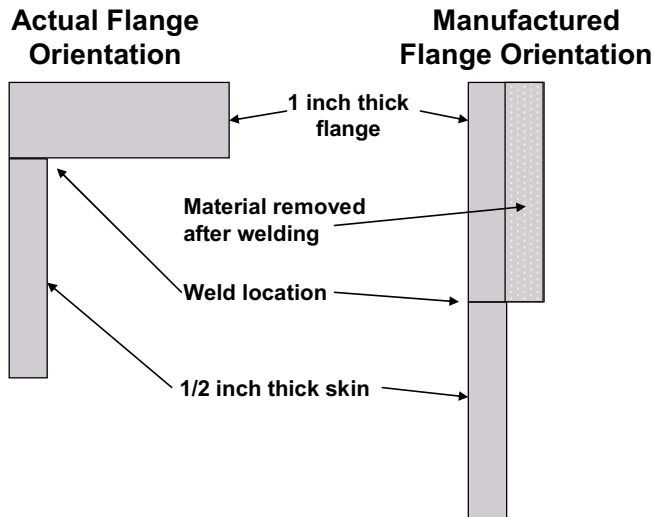


Figure 1. Schematic of weld configuration.

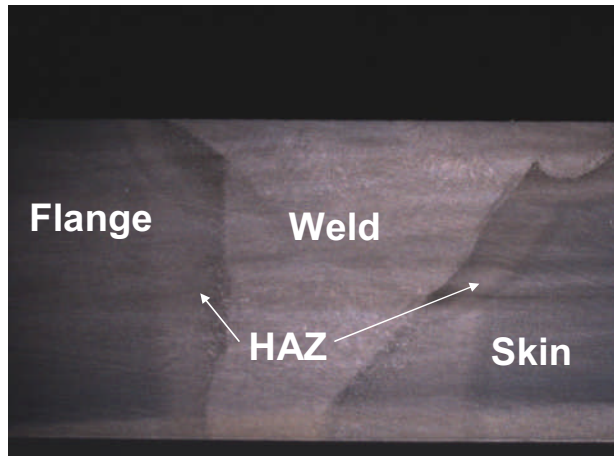


Figure 2. Photograph of an etched cross-section on the single bevel flange-to-skin weld used for the Charpy impact and fracture tests.

Lab Air Fatigue Crack Growth Rate Tests

Fatigue crack growth rate tests were conducted on $\frac{1}{2}$ inch thick A516 Grade 70 steel plates obtained from the same lot of material that was used to construct the USS segments. The fatigue crack growth rate behavior of the weld material was not tested because the weld processes typically do not cause significant changes in the growth rate behavior. Two types of tests were conducted: constant R (the ratio of minimum stress to maximum stress, S_{min}/S_{max}) and threshold tests that were conducted at a constant maximum stress intensity factor (K_{max}) and an increasing stress ratio (R). The constant R tests were conducted for stress ratios of $R=0.3$ and $R=0.7$, as shown in Figure 3. The threshold test was designed to result in a final stress ratio of $R=0.7$ at a stress intensity factor range of $\Delta K = 2 \text{ ksi inch}^{1/2}$.

The test data was used to determine the coefficients to the NASGRO equation [1] given by Equation 1. The exponential parameters p and q were set to 0 to ignore threshold and K_{max} effects. The empirical constants c and n were 6×10^{-10} and 2.8, respectively. The curve fit to the experimental data is shown in Figure 3.

$$\frac{da}{dN} = \frac{c \Delta K^n \left(1 - \frac{\Delta K_{th}}{\Delta K}\right)^p}{\left(1 - \frac{K_{max}}{K_c}\right)^q} \quad (1)$$

Where:

a = crack length

N = number of cycles

da/dN = crack growth rate

c, n, p , and q = empirical constants

ΔK = stress intensity factor range ($K_{max} - K_{min}$)

K_{max} = maximum cyclic stress intensity factor

K_{min} = minimum cyclic stress intensity factor

ΔK_{th} = threshold stress intensity factor range

K_c = critical stress intensity factor

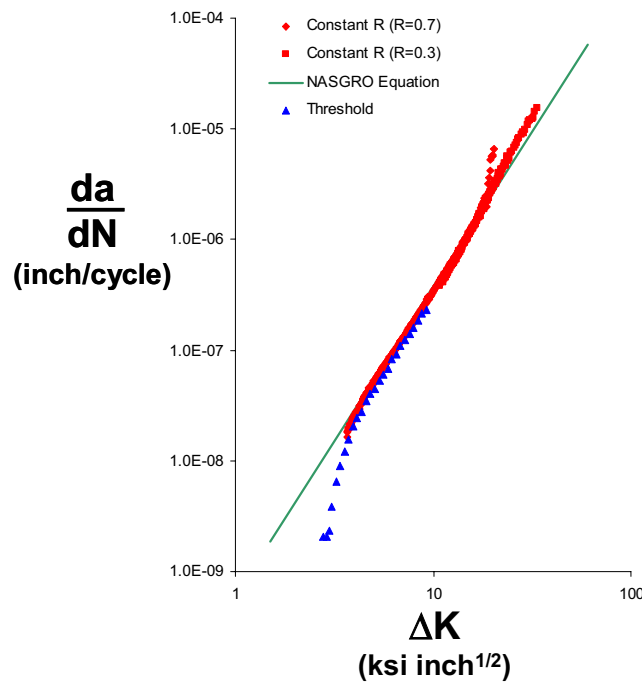


Figure 3. Fatigue crack growth rate test results and the NASGRO curve fit.

Salt Water Fatigue Crack Growth Rate Tests

The Ares I-X USS segments could be exposed to salt water environments in the transportation, rollout, and pad stay segments of the lifetime of the structure. Many steels exhibit accelerated crack

growth rates when exposed to such environments, so a series of tests were conducted to examine the influence, if any, of salt water exposure on the fatigue crack growth rate. Both alternating and full immersion tests were conducted with a 3.5%, by weight, NaCl solution. The alternating immersion tests were conducted under constant ΔK conditions at stress ratio of $R=0.5$ and frequencies of 0.2 and 5 Hz. An eccentrically loaded single edge notch tension ESE(T) specimen was immersed in the solution for 20 minutes, twice per day. The aqueous cell was drained, but not dried after each immersion cycle and the specimen was open to air at all times. Considerable surface corrosion was visible on the specimen, as shown in Figure 4. The specimen was loaded cyclically and measurements of crack length and cycle count were made, as shown in Figure 5. An acceleration of fatigue crack growth would be indicated by a sharp increase in the slope of the crack length against cycle curve. The crack growth rates obtained from the alternating immersion tests did not show any significant acceleration in the fatigue crack growth rate behavior compared to the portion of the test performed in the nominal environment (lab air). The lack of any crack growth rate acceleration may be a result of corrosion by-product induced crack closure that reduced the effective ΔK . Attempts were made to increase the stress ratio, change the stress intensity factor range, and change the frequency, but no accelerated crack growth behavior was observed.

Full immersion fatigue crack growth rate tests were conducted to limit the influence of corrosion by-product induced closure. The full immersion tests were conducted under constant ΔK (12 ksi inch^{1/2}) conditions at a stress ratio of $R=0.5$ and a frequency of 0.2 Hz. The 3.5%, by weight, NaCl solution was deaerated for 40 minutes prior to the introduction of the specimen and inert gas was bubbled through the specimen during the test. The crack growth rate was determined by calculating the slope of the crack length versus cycle test data, but no accelerated behavior was observed, as shown in Figure 6 along with the data from the lab air tests. The full immersion fatigue crack growth rates were actually slower than the lab air tests, providing indirect evidence of corrosion induced closure.



Figure 4. Photograph of corroded single edge crack specimen after being subjected to alternate immersion in a NaCl solution.

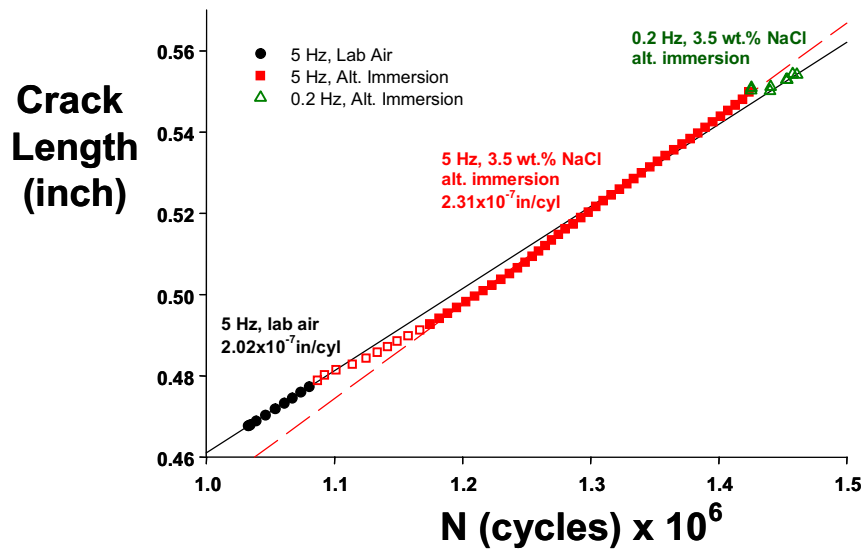


Figure 5. Crack length verses cycle test data for the alternating salt-water solution immersion fatigue crack growth rate tests.

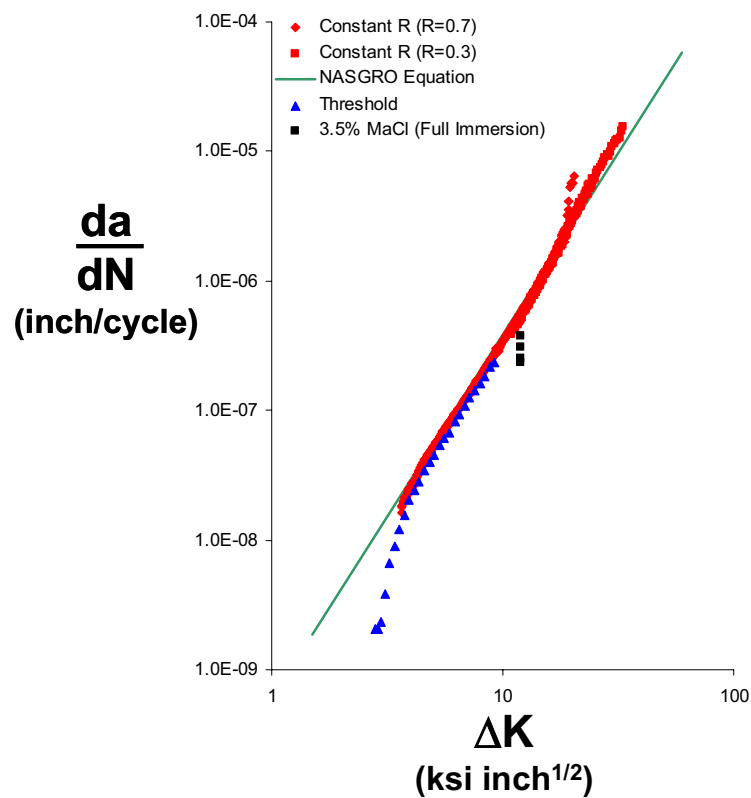


Figure 6. Crack growth rate data for the full salt-water solution immersion fatigue crack growth rate tests and the lab air results.

Charpy Impact Tests

Charpy impact tests were conducted to determine if the potential range of Ares I-X operational temperatures (-20°F to 190°F) would result in a sharp decrease in the fracture behavior. Three duplicate tests were conducted at each of the temperatures of -20°F, 20°F, 60°F, and 190°F. The specimen notch was placed at the interface between the pulse MIG weld and parent materials. The tests conducted at the lower three temperatures were performed with standard size specimens, but the tests at the upper temperature used ½ size specimens and the results were scaled to be equivalent to a full size specimen. The smaller size specimen was used for the high temperature because of the concern that the energy required would exceed the test system capacity. The results indicate that no significant drop in fracture energy was observed for the temperatures tested, as shown in Figure 7. No tests were conducted on specimens made from the flux cored welds.

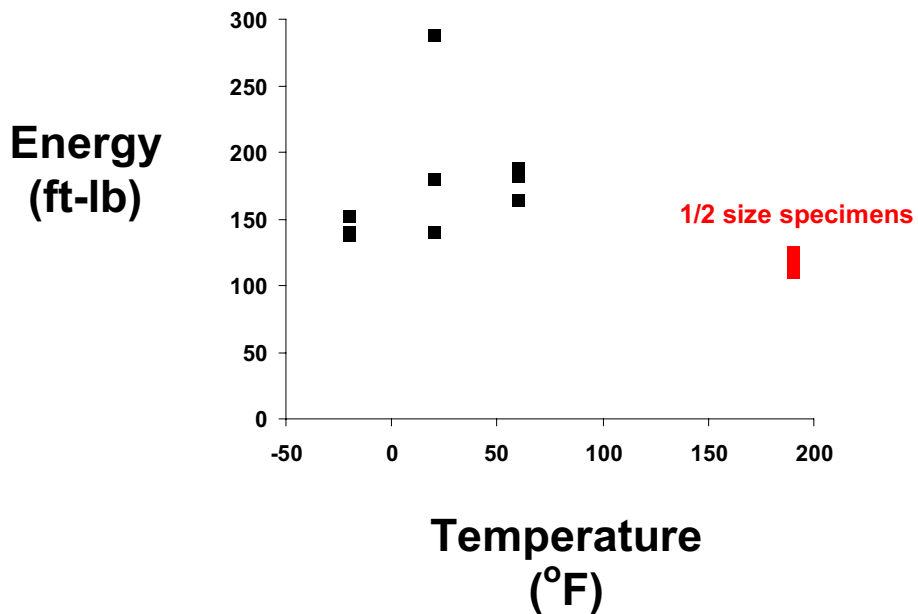


Figure 7. Charpy impact test results.

Fracture Test on Pulse MIG Welds

J_{IC} fracture tests were conducted according to ASTM Standard 1820 [2] for single bevel flange-to-skin welds manufactured using a pulse MIG welding process. Both the flange and skin material were normalized A516 steel. The configuration of the flange-to-skin weld is illustrated in Figure 1 and the orientation of the bevel is shown in Figure 2. The tests were conducted using the automated FTA system [3] for controlling load and displacement, recording crack mouth opening displacement (CMOD), calculating the crack length using compliance measurements, and calculating the J_{IC} values.

The tested configuration was a compact tension (CT) specimen ($W = 3$ inches), as shown in Figure 8. The CT specimens were machined flat and parallel after the weld process to remove any distortion due to welding process. This resulted in a variation of specimen thickness that ranged from

0.43 to 0.48 inches. Each specimen was measured and the actual thickness was used in the J_{IC} calculations.

The specimens were precracked at a stress intensity factor range of $\Delta K = 11.5 \text{ ksi inch}^{1/2}$ and a stress ratio of $R=0.3$. The initial ratio of notch length to specimen width was $a/W = 0.46$ and the ratio of crack length to width after precracking was between $a/W=0.48$ and 0.50. A 90° side groove was machined into each specimen after precracking to promote straight crack growth during the fracture process.

An etched through-the-thickness cross section of the weld is shown in Figure 9. The etching reveals interfaces between the parent material and heat affected zone (HAZ) and between the HAZ and the weld. The CT specimens were machined to allow the notch to coincide with one of the three locations (A, B, and C). Location A is located 0.04 inches from the intersection of the weld and the HAZ at the narrow end of the bevel and places the notch in the HAZ. Location B is located at the interface of the weld and the HAZ at the narrow end of the bevel. Location C is located in the weld material.

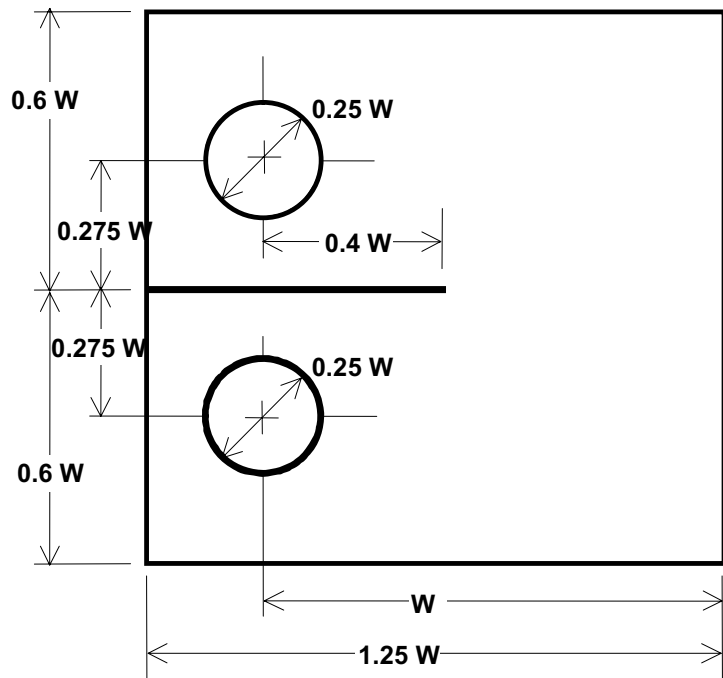


Figure 8. Compact tension specimen used in the pulse MIG weld fracture tests.

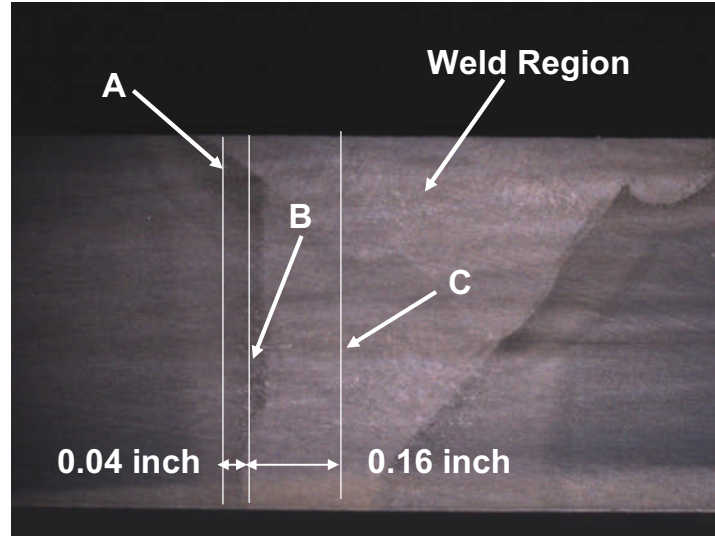


Figure 9. Location of the notch in the CT specimen relative to the weld.

The CT specimens were loaded in displacement control and the CMOD was measured with an extensometer attached to the front edge of the specimen, centered about the notch. The displacement was monotonically increased at a rate of 0.02 inches/minute with unloading cycles performed every 0.003 inches of displacement or every 500 lbs of load increase. The unloading cycles decreased the load 1000 lbs. less than that at the start of the unloading. Visual crack length measurements were not performed because the side grooves prevented accurate crack length measurements. Instead, the crack length measurements were estimated from the CMOD measurements. The J_{IC} value and the elastic component of the J_{IC} was calculated according to ASTM Standard 1820 [2] for each test using the FTA system, a computer-controlled automated crack growth system using a servo-hydraulic test machine [3]. An example of the output from the FTA system for a J_{IC} test is shown in Figure 10. The J_{IC} value is the J-integral at the start of stable tearing and is shown by the green symbol in Figure 10.

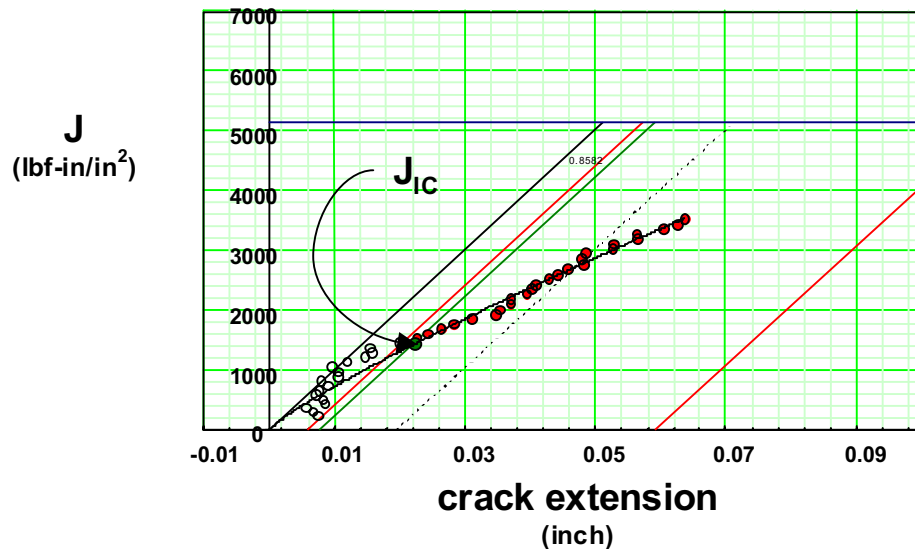


Figure 10. The J_{IC} calculation from the FTA system for a CT specimen with the notch at location B.

Six fracture tests were conducted for each of the three locations. The results from the fracture tests are shown in Figure 11 in terms of the J-R (J-integral against crack extension). The blue data points represent tests conducted with the notch placed in the HAZ (Location A). The red points represent tests conducted with the notch placed at the interface between the weld and the HAZ (Location B). The green points represent tests conducted with the notch in the weld region (Location C). The CT specimens with the notch placed at Location B had the lowest values of the J-integral for a given amount of crack extension. The J_{IC} and the elastic component of the J_{IC} are shown in Table 1 and the average values and standard deviation for the three sets of fracture test results are shown in Table 2. The tests conducted with the notch placed at the interface between the weld and the HAZ had the lowest values of J_{IC} . The elastic component of the J_{IC} was very similar in value for all three locations.

The fracture tests violated the crack front shape criterion of ASTM Standard 1820 [2] because considerable variation through-the-thickness was observed in every test, as illustrated by the example shown in Figure 12. Additional photographs of the weld and parent fracture surfaces are provided in the Appendix.

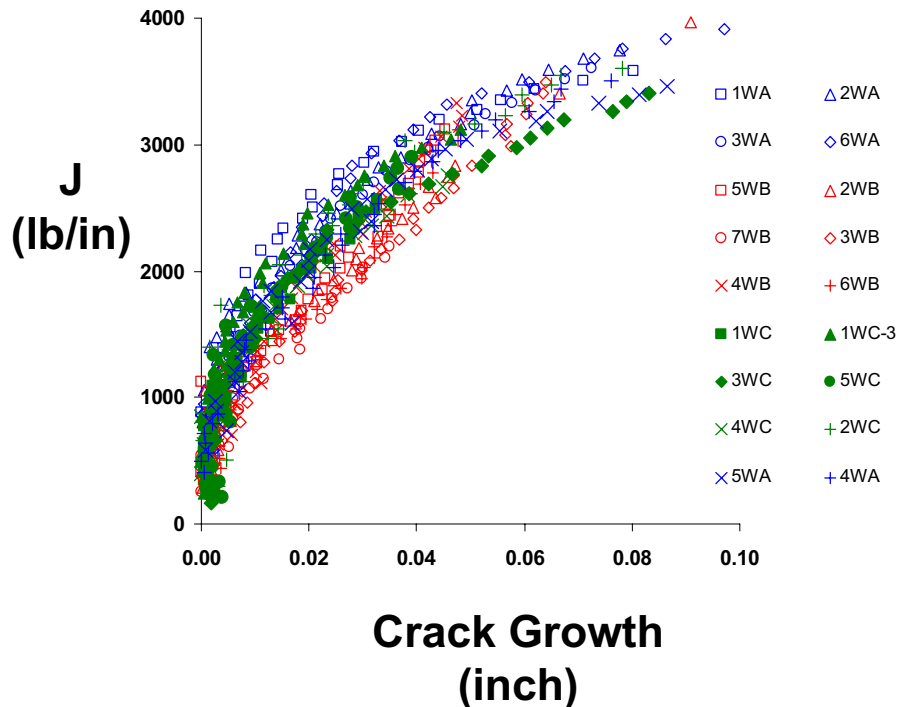


Figure 11. Fracture test results from the pulse MIG weld material

Table 1. Results from the Fracture Tests Conducted on the A516 Steel with the Pulse MIG Welds

Specimen	J_{IC} (lb/in)	J_{ICelastis} (lb/in)
1WA	3040	389
2WA	2727	411
3WA	2651	418
5WA	2236	396
4WA	2067	403
6WA	2980	433
3WB	1527	382
7WB	1456	375
2WB	1703	389
5WB	1555	396
4WB	2202	433
6WB	1456	382
1WC	2202	375
1WC-3	2823	389
3WC	2412	375
5WC	2448	382
4WC	2185	389
2WC	2708	411

Table 2. Average and Standard Deviation for the Fracture Tests Conducted on the A516 Steel with the Pulse MIG Welds

Location	Average J_{IC} (lb/in)	Std Dev J_{IC} (lb/in)	Average J_{ICelastis} (lb/in)	Std Dev J_{ICelastis} (lb/in)
A	2617	393	408	16
B	1650	285	393	21
C	2463	387	387	13



Figure 12. Photograph of the fracture surface of a pulse MIG weld.

Fracture Test on Flux-cored Welds

J_{IC} fracture tests were conducted according to ASTM Standard 1820 [2] for single bevel flange-to-skin welds manufactured using flux-cored welding process. Both the flange and skin material were normalized A516 Grade 70 steel. The configuration of the flange-to-skin weld was the same as described for the pulse MIG fracture tests. The tests were conducted using the automated FTA system [3] for controlling load and displacement, recording crack mouth opening displacement (CMOD), calculating the crack length using compliance measurements, and calculating the J_{IC} values.

The specimen configuration was a 2-inch wide compact tension (CT) specimen ($W = 2$ inches in Figure 8). The CT specimens were machined flat and parallel after the weld process to remove any distortion due to welding. This resulted in a variation of specimen thickness that ranged from 0.45 to 0.49 inches. Each specimen was measured and the actual thickness was used in the J_{IC} calculations.

The specimens were precracked at a stress intensity factor range of $\Delta K = 10$ ksi inch $^{1/2}$ and a stress ratio of $R=0.3$. The initial ratio of notch length to specimen width was $a/W = 0.45$ and the ratio of crack length to width after precracking was between $a/W = 0.49$ and 0.50. A 90° side groove was machined into each specimen after precracking to promote straight crack growth during the fracture process.

The CT specimens were machined to allow the notch to coincide with one of the four locations (HAZ, weld, parent 0°, and parent 90°). The HAZ location was identical to Location B of the pulse MIG fracture specimens and was located at the interface of the weld and the HAZ at the narrow end of the bevel. The weld location was identical to Location C of the pulse MIG fracture specimens and was located in the weld material. The parent 0° location was away from the weld and HAZ with the notch parallel to the weld. The parent 90° location was away from the weld and HAZ with the notch perpendicular to the weld.

The CT specimens were loaded in displacement control and the CMOD was measured with an extensometer attached to knife edges machined into the specimen, centered about the notch and in line with the center of the pin holes. The displacement was monotonically increased at a rate of 0.02 inches/minute with unloading cycles performed every 0.003 inches of displacement or every 500 lbs of load increase. The unloading cycles decreased the load 1000 lbs less than that at the start of the unloading. Visual crack length measurements were not performed because the side grooves prevented accurate crack length measurements. Instead, the crack length measurements were estimated from the CMOD measurements. The J_{IC} value and the elastic component of the J_{IC} was calculated according to ASTM Standard 1820 [2] for each test using the automated computer-controlled FTA system [3]. An example of the output from the FTA system for a J_{IC} test is shown in Figure 13. The J_{IC} value is the J-integral at the start of stable tearing and is shown by the green symbol in Figure 13.

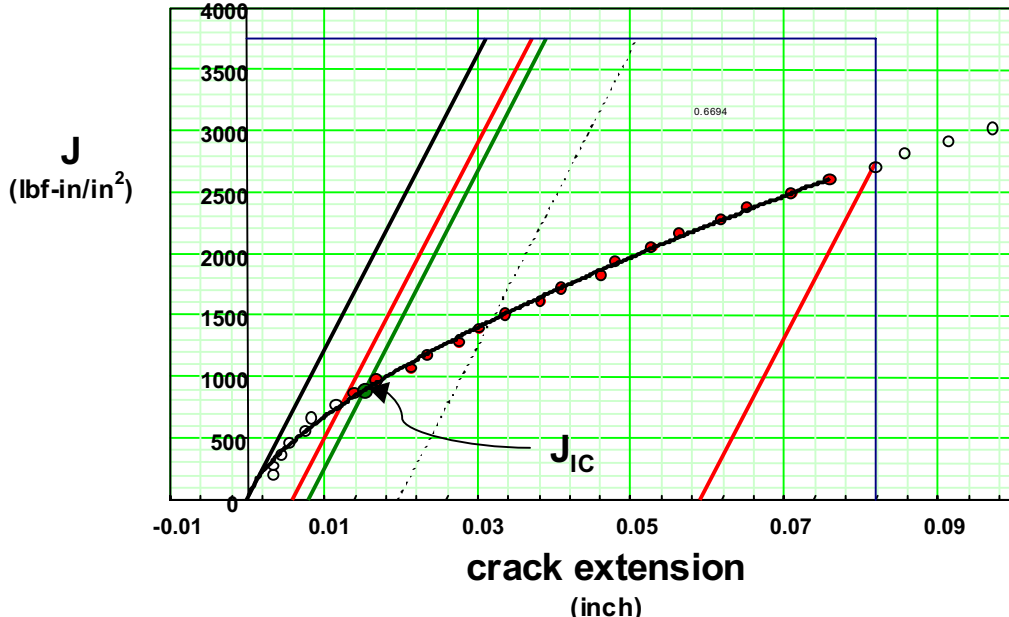


Figure 13. The J_{IC} calculation from the FTA system for a CT specimen with the notch in the weld material.

Three fracture tests were conducted for each of the four locations. The results from the fracture tests are shown in Figure 14 in terms of the J -R (J -integral against crack extension). The blue, red, green, and purple data points represent tests conducted with the notch placed in the HAZ, weld material, parent material parallel to the direction of the weld (parent 0°), and parent material perpendicular to the direction of the weld (parent 90°), respectively. The CT specimens with the notch placed in the weld had the lowest values of the J -integral for a given amount of crack extension. The J_{IC} and the elastic component of the J_{IC} are shown in Table 3 and the average values and standard deviation for the four sets of fracture test results are shown in Table 4. The tests conducted with the notch placed in the weld material had the lowest values of J_{IC} while the parent material tests had lower values of elastic component of the J_{IC} .

Each specimen was heated to 500°F for approximately 30 minutes to heat tint the cracked specimens. The heat tinting caused the fracture surfaces to turn different colors depending on loading that was growing the crack and allowed for easy determination of the final crack configuration, as shown in Figure 15. The notch region was turned a rusty red color, the fatigue precrack region was turned a light blue color, and the fracture region was turned a dark blue. The specimens were pulled to failure after the specimen was cooled and the subsequent fracture surface had a very light color. The fracture tests violated the crack front shape criterion of ASTM Standard 1820 [3] because considerable variation through-the-thickness was observed in every tests, as shown in Figure 15.

Two CT specimens had internal defects in the weld region that were revealed after the specimens have been fractured. Specimen A2 (notch placed in the weld region) had a $1/8$ inch long by $1/16$ inch wide slag inclusion along the mid-thickness, as shown in Figure 16. This defect was more than $1/2$ inch away from the fracture region in the test. Specimen C2 had a similar sized defect that was located in the fracture region, as shown in Figure 17.

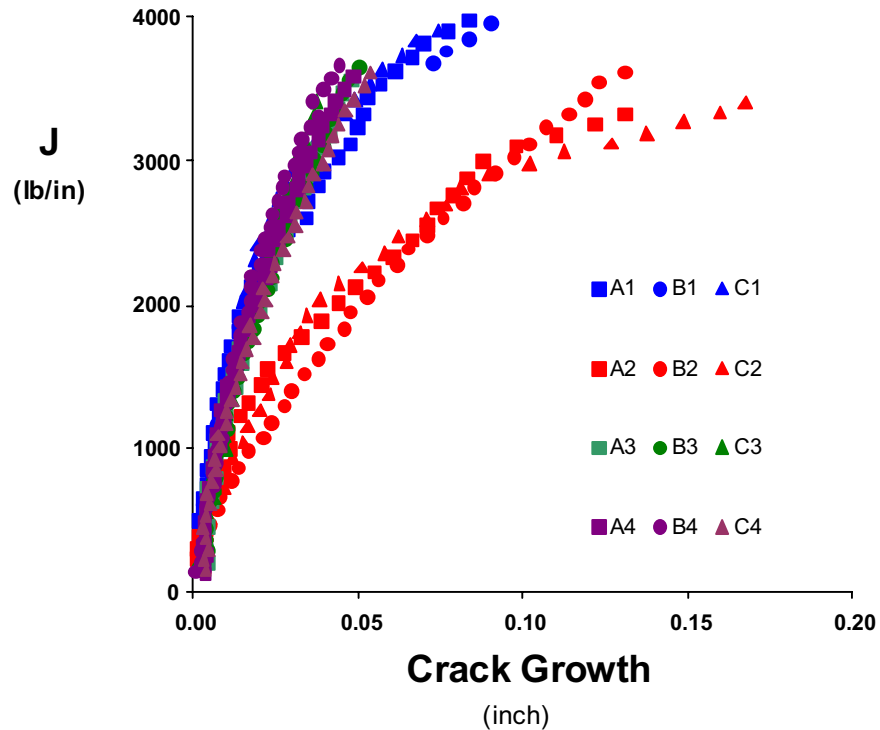


Figure 14. Fracture test results from the flux cored weld material

Table 3. Results from the Fracture Tests Conducted on the A516 Steel with the Flux Cored Welds

Location	Specimen	J_{IC} (lb/in)	$J_{ICelast}$ (lb/in)
HAZ	A1	2491	297
HAZ	B1	2805	299
HAZ	C1	3022	326
Weld	A2	1403	332
Weld	B2	892	292
Weld	C2	1230	325
Parent 0°	A3	2617	265
Parent 0°	B3	2583	258
Parent 0°	C3	3191	279
Parent 90°	A4	2835	231
Parent 90°	B4	3201	242
Parent 90°	C4	2437	226

Table 4. Average and Standard Deviation for the A516 Steel Fracture Tests with the Flux Cored Welds

Location	Average J_{IC} (lb/in)	Std Dev J_{IC} (lb/in)	Average $J_{ICelastic}$ (lb/in)	Std Dev $J_{ICelastic}$ (lb/in)
HAZ	2773	267	307	16
Weld	1175	260	316	21
Parent 0°	2797	342	267	11
Parent 90°	2824	382	233	8

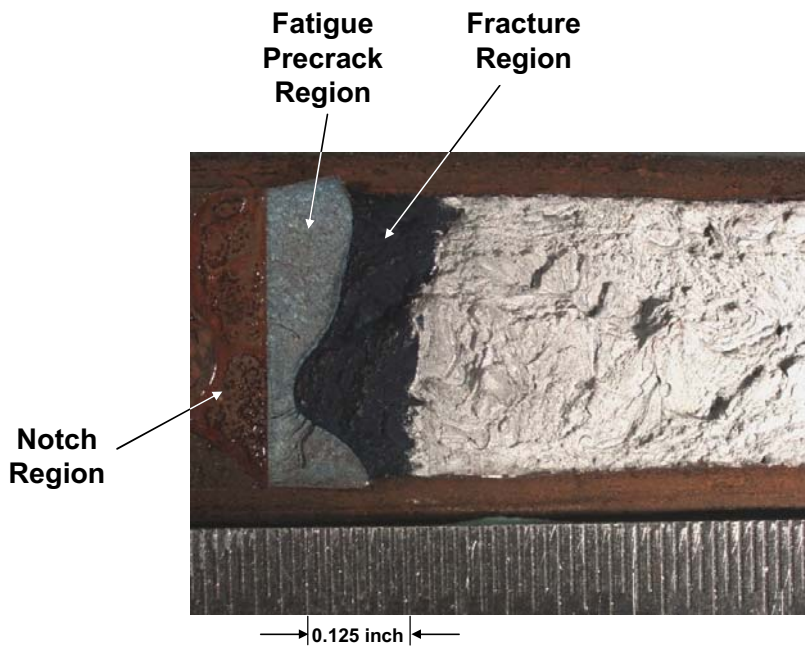


Figure 15. Photograph of the fracture surface of a flux cored weld.

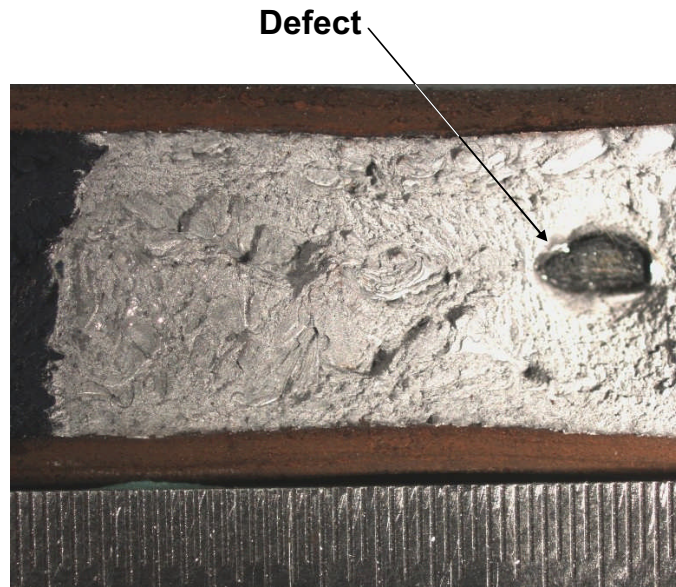


Figure 16. Photograph of the fracture surface of a flux cored weld with a defect ahead of the crack front.

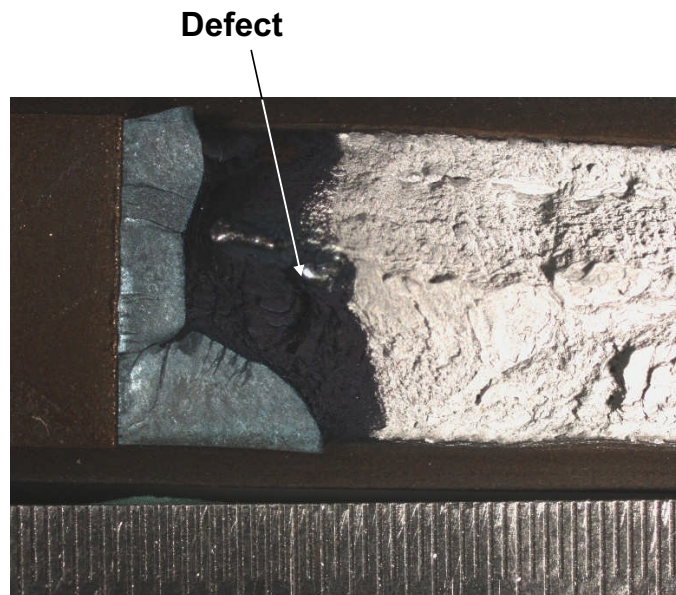


Figure 17. Photograph of the fracture surface of a flux cored weld with a defect in the fracture region.

The measured elastic component of the J_{IC} was converted into a critical stress intensity factor (K_c), using the relationship given in Equation 2. A 0.1/90% lower bound was calculated for the critical stress intensity factors using Equation 3. The weld location had the lowest 0.1/90% tolerance critical stress intensity factor as shown in Table 5.

$$K_c = \sqrt{J_{ICelastic} E} \quad (2)$$

Where:

E is the elastic modulus (30,000,000 psi for A516 steel)

$$K_{c0.1/90} = \bar{K}_c - k_n \times s \quad (3)$$

Where:

$K_{c0.1/90}$ is the 0.1/90% lower bound critical stress intensity factor

\bar{K}_c is the average critical stress intensity factor results

s is the standard deviation for the critical stress intensity factor results

k_n is the normal distribution sample size factor (9.651 for three samples)

Table 5. 0.1/90% Lower Bound Critical Stress Intensity Factor

Location	Avg K_c (ksi inch ^{1/2})	Std Dev K_c (ksi inch ^{1/2})	0.1/90% K_c (ksi inch ^{1/2})
HAZ	96.0	2.5	72
Weld	97.4	3.3	65
Parent 0°	89.5	1.8	72
Parent 90°	83.6	1.5	69

Conclusions

An independent assessment was conducted to determine the critical initial flaw size (CIFS) for the flange-to-skin weld in the Ares I-X Upper Stage Simulator (USS). The material behavior parameters required for the CIFS analyses were obtained by conducting fatigue crack growth rate, Charpy impact, and fracture tests. The material that was investigated was parent and welded A516 Grade 70 steel from the same lot of material used to manufacture the Ares I-X USS segments. The tested weld processes were performed by the welders working on the flight hardware and using the current flight weld procedures. However, the flight weld process changed after the tests were conducted, resulting in uncertainty between the similitude of the tested critical fracture toughness and that of the flight welds.

The crack growth rate tests confirmed that the crack growth performance was in agreement with literature data, and that a salt water environment would not significantly degrade the fatigue crack growth resistance. The Charpy impact tests confirmed that the fracture resistance of the material did not have a significant reduction for the expected operational temperatures of the vehicle (-20°F to 190°F). Finally, the fracture toughness tests revealed that a fracture toughness (K_c) value of 65 ksi inch^{1/2} was appropriate for this material.

References

1. Forman, R. G., Shivakumar, V., and Newman, J. C., Jr. "Fatigue crack growth computer program NASA/FLAWGRO," Technical Report JSC-22267A, NASA 1993.
2. "Annual Book of ASTM Standards", Standard E1820, Volume 03.01, 2006.
3. Donald, K., "Non-Linear Fracture Toughness Testing – Series 2003," FTA Users Guide.

Appendix: Test Measurements and Data

The following tables and figures contain the test measurements and data for the tests that were described above.

Table A-1. Crack Growth Rate Data for the Threshold Tests on the Normalized A516 Steel

Crack Length (inch)	Cycle Count	ΔK (ksi in ^{1/2})	da/dN (in/cycle)
1.168405	15862	9.70389	2.27E-07
1.172667	33359	9.25256	2.32E-07
1.177533	55202	8.80903	2.15E-07
1.182944	81091	8.38802	1.83E-07
1.187849	111487	7.95528	1.61E-07
1.193252	145284	7.56983	1.41E-07
1.198161	184751	7.18678	1.25E-07
1.203401	226681	6.84043	1.09E-07
1.208128	276007	6.50131	9.24E-08
1.213296	333812	6.19911	8.32E-08
1.217907	393542	5.90219	6.78E-08
1.222666	472060	5.60207	6.03E-08
1.228491	569004	5.34713	5.34E-08
1.233178	669105	5.06435	4.5E-08
1.238077	781999	4.81481	4.03E-08
1.243711	930645	4.58102	3.45E-08
1.248732	1091075	4.35227	2.79E-08
1.253247	1272894	4.13416	2.43E-08
1.258532	1495116	3.9448	2.05E-08
1.263276	1762792	3.75012	1.56E-08
1.268041	2106227	3.56788	1.21E-08
1.27323	2586025	3.39689	9.02E-09
1.278241	3237540	3.22497	6.58E-09
1.283401	4131479	3.08095	3.82E-09
1.28744	5646633	2.96625	2.35E-09
1.289638	6788048	2.87816	2.06E-09
1.291643	7692088	2.79635	2.08E-09

Table A-2. Crack Growth Rate Data for the R=0.3 Tests on the Normalized A516 Steel

Crack Length (inch)	Cycle Count	ΔK (ksi in ^{1/2})	da/dN (in/cycle)	Crack Length (inch)	Cycle Count	ΔK (ksi in ^{1/2})	da/dN (in/cycle)	Crack Length (inch)	Cycle Count	ΔK (ksi in ^{1/2})	da/dN (in/cycle)
1.312799	33176	10.7614	3.9E-07	1.57509	518414	13.95913	8.21E-07	1.836736	718122	19.12262	2.38E-06
1.317979	46490	10.80975	3.83E-07	1.579956	523955	14.03045	8.66E-07	1.841995	720201	19.25648	2.57E-06
1.322834	59385	10.86036	3.86E-07	1.585102	529978	14.10868	8.56E-07	1.847221	722201	19.39386	2.61E-06
1.327782	71856	10.91054	4.1E-07	1.590469	536242	14.18612	8.88E-07	1.852404	724184	19.5226	2.65E-06
1.332897	83908	10.95964	4.21E-07	1.595366	541542	14.26251	9.03E-07	1.856882	725849	19.66118	2.76E-06
1.337637	95239	11.01197	4.16E-07	1.599825	546601	14.33954	9.05E-07	1.862025	727673	19.78368	2.76E-06
1.342776	107676	11.06304	4.22E-07	1.604737	551901	14.41612	9.32E-07	1.866524	729338	19.91655	2.85E-06
1.347961	119731	11.11599	4.32E-07	1.609932	557442	14.4948	9.34E-07	1.871107	730856	20.04958	2.87E-06
1.353059	131498	11.16959	4.24E-07	1.614868	562742	14.57509	9.56E-07	1.876152	732687	20.18592	2.93E-06
1.358138	143737	11.22096	4.15E-07	1.61961	567560	14.65806	9.88E-07	1.88129	734328	20.32358	3.11E-06
1.362827	155034	11.27325	4.29E-07	1.624864	572860	14.73837	9.92E-07	1.885954	735843	20.47573	3.26E-06
1.36763	165860	11.32422	4.37E-07	1.629883	577919	14.82094	1.04E-06	1.891369	737422	20.61642	3.38E-06
1.372503	177157	11.37695	4.47E-07	1.634571	582210	14.90183	1.02E-06	1.896398	738937	20.76542	3.21E-06
1.377522	187983	11.43008	4.61E-07	1.63921	587033	14.98361	1.02E-06	1.901086	740452	20.91839	3.28E-06
1.382474	198809	11.48662	4.76E-07	1.64417	591663	15.0648	1.09E-06	1.906323	741967	21.06762	3.45E-06
1.387832	209636	11.53933	4.72E-07	1.649054	596100	15.15035	1.12E-06	1.911535	743482	21.21983	3.48E-06
1.392481	219991	11.59564	4.58E-07	1.654321	600731	15.23476	1.12E-06	1.916215	744808	21.37667	3.71E-06
1.397315	230347	11.65061	4.95E-07	1.658814	604782	15.3232	1.12E-06	1.921191	746083	21.53049	3.97E-06
1.402509	240232	11.70033	4.91E-07	1.663618	609027	15.40864	1.14E-06	1.92629	747346	21.6805	3.89E-06
1.406554	249175	11.7583	4.82E-07	1.668752	613464	15.49652	1.17E-06	1.930822	748558	21.84129	3.74E-06
1.411591	259063	11.81257	5.16E-07	1.673757	617709	15.58934	1.19E-06	1.935744	749871	21.99396	3.87E-06
1.417093	269613	11.87066	5.1E-07	1.678879	621953	15.67897	1.22E-06	1.940606	751084	22.15955	4.31E-06
1.422154	279785	11.9309	5E-07	1.683686	625812	15.7678	1.25E-06	1.945771	752195	22.32271	4.35E-06
1.427081	289581	11.98756	4.97E-07	1.688174	629402	15.85959	1.26E-06	1.950718	753407	22.49715	4.27E-06
1.431713	299000	12.04694	5.21E-07	1.693238	633421	15.95195	1.27E-06	1.955903	754568	22.66512	4.55E-06
1.436898	308420	12.10454	5.45E-07	1.698539	637593	16.04563	1.28E-06	1.960825	755629	22.84397	4.64E-06
1.441986	317839	12.16434	5.26E-07	1.703343	641302	16.14091	1.32E-06	1.965983	756740	23.01703	4.88E-06
1.446615	327258	12.22461	5.51E-07	1.707939	644702	16.23807	1.35E-06	1.970928	757699	23.18414	4.89E-06
1.451749	335547	12.28293	5.85E-07	1.713165	648566	16.33517	1.39E-06	1.975223	758629	23.3555	4.66E-06
1.456511	343836	12.34533	5.8E-07	1.718467	652275	16.42811	1.39E-06	1.979786	759598	23.53481	5.35E-06
1.461809	352878	12.40348	5.86E-07	1.722629	655366	16.53268	1.37E-06	1.985391	760528	23.70757	5.61E-06
1.46644	360790	12.46412	5.87E-07	1.727789	659075	16.63105	1.47E-06	1.990208	761457	23.9049	5.4E-06
1.470928	368402	12.52661	6E-07	1.733343	662630	16.72789	1.51E-06	1.995202	762346	24.08221	5.15E-06
1.476253	377147	12.58825	5.96E-07	1.737685	665629	16.84314	1.57E-06	1.999789	763316	24.28524	5.38E-06
1.481534	386192	12.65228	6.04E-07	1.743289	668970	16.94043	1.59E-06	2.00543	764246	24.51559	6.11E-06
1.486264	393730	12.71249	6.1E-07	1.748282	672311	17.0507	1.59E-06	2.012658	765423	24.82436	6.05E-06
1.490361	400664	12.77819	6.32E-07	1.753145	675157	17.15128	1.71E-06	2.022689	767099	25.17332	6.21E-06
1.495792	408805	12.83754	6.52E-07	1.757577	677756	17.26046	1.67E-06	2.03264	768640	25.58127	6.71E-06
1.50078	416646	12.90717	6.47E-07	1.76287	680973	17.36279	1.62E-06	2.042344	770029	26.00636	7.09E-06
1.505941	424485	12.97408	6.66E-07	1.767828	684066	17.47305	1.64E-06	2.052339	771417	26.44703	7.53E-06
1.511014	432022	13.03986	6.61E-07	1.772587	686912	17.58553	1.78E-06	2.062785	772743	26.91231	7.96E-06
1.515699	439258	13.10774	6.53E-07	1.777719	689634	17.68995	1.89E-06	2.073442	774069	27.37876	8.27E-06
1.520661	446796	13.17567	6.95E-07	1.782287	692035	17.8049	1.88E-06	2.083152	775205	27.8596	8.94E-06
1.525967	454033	13.2447	7.33E-07	1.787252	694708	17.91268	1.87E-06	2.09263	776215	28.32494	9.28E-06
1.531045	460968	13.31315	7.12E-07	1.792085	697282	18.03042	1.88E-06	2.101935	777229	28.80984	9.19E-06
1.535625	467601	13.38295	7.14E-07	1.797289	700054	18.14752	1.89E-06	2.111692	778290	29.31415	9.84E-06
1.540513	474234	13.45095	7.36E-07	1.802419	702751	18.26641	2.08E-06	2.121821	779249	29.84279	1.09E-05
1.545605	481169	13.52088	7.71E-07	1.807265	704855	18.38621	2.22E-06	2.131908	780138	30.40909	1.15E-05
1.550504	487199	13.58766	7.91E-07	1.812126	707133	18.51118	2.17E-06	2.142355	781029	30.97358	1.19E-05
1.554759	492743	13.66384	7.72E-07	1.817579	709608	18.63098	2.23E-06	2.152219	781838	31.55578	1.23E-05
1.560368	499971	13.73509	7.75E-07	1.822494	711786	18.75387	2.25E-06	2.161705	782605	32.14837	1.27E-05
1.565872	507082	13.81267	8.13E-07	1.826952	713766	18.87414	2.25E-06	2.171517	783357	32.77745	1.43E-05
1.570807	512810	13.88559	8.13E-07	1.831609	715845	18.99517	2.25E-06	2.182273	784039	33.37965	1.53E-05

Table A-3. Crack Growth Rate Data for the R=0.7 Tests on the Normalized A516 Steel

ΔK (ksi) in ^{1/2}	da/dN (in/cycle)										
1.79E-08	3.65257	4.12E-08	4.6348	7.62E-08	5.76473	1.43E-07	7.28742	2.93E-07	9.58333	8.16E-07	13.46093
1.64E-08	3.66789	4.20E-08	4.65527	7.71E-08	5.79037	1.45E-07	7.3241	3.01E-07	9.64117	8.31E-07	13.56342
1.85E-08	3.68279	4.17E-08	4.67542	7.88E-08	5.81577	1.48E-07	7.3618	3.08E-07	9.70021	8.34E-07	13.66923
1.92E-08	3.70171	4.23E-08	4.69625	8.00E-08	5.84142	1.50E-07	7.39922	3.13E-07	9.76058	8.45E-07	13.77782
1.96E-08	3.71939	4.45E-08	4.7166	7.96E-08	5.86709	1.52E-07	7.43677	3.22E-07	9.82148	8.57E-07	13.88537
1.99E-08	3.73692	4.51E-08	4.73728	8.02E-08	5.89309	1.53E-07	7.47361	3.32E-07	9.88338	8.87E-07	13.9946
2.01E-08	3.75463	4.61E-08	4.75792	8.18E-08	5.91964	1.55E-07	7.51084	3.38E-07	9.94431	9.34E-07	14.10507
2.07E-08	3.77223	4.68E-08	4.77841	8.32E-08	5.94646	1.58E-07	7.54879	3.43E-07	10.00607	9.68E-07	14.21533
2.15E-08	3.79012	4.61E-08	4.7994	8.40E-08	5.97357	1.61E-07	7.58792	3.47E-07	10.069	9.75E-07	14.32767
2.18E-08	3.8079	4.65E-08	4.82001	8.45E-08	6.00077	1.62E-07	7.62736	3.53E-07	10.13235	9.88E-07	14.44471
2.12E-08	3.82554	4.74E-08	4.84078	8.64E-08	6.02793	1.65E-07	7.66766	3.61E-07	10.19734	1.02E-06	14.56108
2.17E-08	3.84359	4.85E-08	4.86219	8.76E-08	6.05535	1.68E-07	7.70793	3.67E-07	10.26269	1.04E-06	14.67948
2.28E-08	3.86113	4.86E-08	4.88304	8.78E-08	6.08298	1.70E-07	7.74836	3.72E-07	10.32831	1.06E-06	14.80012
2.31E-08	3.87918	4.81E-08	4.90442	8.85E-08	6.1107	1.72E-07	7.78971	3.78E-07	10.39419	1.09E-06	14.92186
2.39E-08	3.89722	4.94E-08	4.92605	9.00E-08	6.13857	1.74E-07	7.8299	3.87E-07	10.46132	1.12E-06	15.04626
2.46E-08	3.91507	5.09E-08	4.94701	9.21E-08	6.1669	1.76E-07	7.87106	3.94E-07	10.52811	1.15E-06	15.17215
2.50E-08	3.93338	5.08E-08	4.96813	9.26E-08	6.19508	1.78E-07	7.91199	4.02E-07	10.59504	1.18E-06	15.29582
2.47E-08	3.95138	5.14E-08	4.9897	9.34E-08	6.2234	1.82E-07	7.95434	4.07E-07	10.66301	1.22E-06	15.42188
2.38E-08	3.9694	5.25E-08	5.01101	9.52E-08	6.25193	1.84E-07	7.99707	4.15E-07	10.73177	1.26E-06	15.54809
2.44E-08	3.98749	5.32E-08	5.03295	9.57E-08	6.28036	1.85E-07	8.04028	4.23E-07	10.80233	1.30E-06	15.68124
2.56E-08	4.00539	5.33E-08	5.05485	9.59E-08	6.30916	1.89E-07	8.08413	4.29E-07	10.87482	1.34E-06	15.81592
2.65E-08	4.02343	5.31E-08	5.07671	9.79E-08	6.3387	1.93E-07	8.12704	4.40E-07	10.94845	1.37E-06	15.95351
2.74E-08	4.04177	5.40E-08	5.09828	9.97E-08	6.36853	1.96E-07	8.17067	4.49E-07	11.02183	1.41E-06	16.09377
2.83E-08	4.12586	5.55E-08	5.12034	1.01E-07	6.39854	1.99E-07	8.21413	4.57E-07	11.09675	1.44E-06	16.23108
2.67E-08	4.13643	5.64E-08	5.14233	1.02E-07	6.42877	2.03E-07	8.25826	4.68E-07	11.17156	1.47E-06	16.37339
2.76E-08	4.15279	5.73E-08	5.16503	1.03E-07	6.45839	2.06E-07	8.30298	4.77E-07	11.24728	1.52E-06	16.51639
2.93E-08	4.17102	5.85E-08	5.18758	1.04E-07	6.48852	2.08E-07	8.34803	4.87E-07	11.3227	1.58E-06	16.66289
2.93E-08	4.1902	5.84E-08	5.21026	1.06E-07	6.51898	2.11E-07	8.39491	4.92E-07	11.39913	1.65E-06	16.81168
2.93E-08	4.2088	5.82E-08	5.23341	1.08E-07	6.54945	2.14E-07	8.4409	4.98E-07	11.47572	1.70E-06	16.96212
2.99E-08	4.22772	5.91E-08	5.25612	1.09E-07	6.58064	2.18E-07	8.48815	5.07E-07	11.55483	1.76E-06	17.11617
3.13E-08	4.24653	5.93E-08	5.27895	1.10E-07	6.6116	2.21E-07	8.53628	5.17E-07	11.63711	1.84E-06	17.27137
3.19E-08	4.26534	6.05E-08	5.30218	1.11E-07	6.64316	2.23E-07	8.58361	5.30E-07	11.71786	1.94E-06	17.42792
3.22E-08	4.28445	6.23E-08	5.32489	1.13E-07	6.67467	2.27E-07	8.63197	5.40E-07	11.80148	2.00E-06	17.5861
3.25E-08	4.30323	6.22E-08	5.34822	1.15E-07	6.70686	2.30E-07	8.68007	5.52E-07	11.88435	2.07E-06	17.74716
3.34E-08	4.32216	6.28E-08	5.37204	1.16E-07	6.73907	2.33E-07	8.7298	5.64E-07	11.96734	2.19E-06	17.90996
3.41E-08	4.34103	6.37E-08	5.39538	1.18E-07	6.77117	2.36E-07	8.77908	5.77E-07	12.05398	2.27E-06	18.07827
3.40E-08	4.36022	6.47E-08	5.41916	1.20E-07	6.80417	2.39E-07	8.82909	5.93E-07	12.13912	2.37E-06	18.24838
3.45E-08	4.37925	6.59E-08	5.44305	1.22E-07	6.83693	2.43E-07	8.8799	6.04E-07	12.22611	2.47E-06	18.41745
3.52E-08	4.39858	6.71E-08	5.46692	1.23E-07	6.87044	2.49E-07	8.93021	6.15E-07	12.31361	2.00E-06	18.57149
3.58E-08	4.41799	6.85E-08	5.49101	1.23E-07	6.90353	2.53E-07	8.98155	6.28E-07	12.40083	2.25E-06	18.77175
3.65E-08	4.43753	6.92E-08	5.51516	1.25E-07	6.93681	2.57E-07	9.03448	6.42E-07	12.49038	3.21E-06	18.93227
3.71E-08	4.45699	6.96E-08	5.53911	1.27E-07	6.97042	2.62E-07	9.08787	6.56E-07	12.58093	3.57E-06	19.13602
3.77E-08	4.4766	7.06E-08	5.56352	1.28E-07	7.00439	2.67E-07	9.1411	6.66E-07	12.67444	4.15E-06	19.32596
3.81E-08	4.496	7.08E-08	5.58804	1.30E-07	7.03899	2.70E-07	9.1952	6.80E-07	12.76875	5.31E-06	19.50716
3.88E-08	4.51554	7.13E-08	5.61263	1.32E-07	7.07348	2.73E-07	9.24847	6.98E-07	12.86408	5.67E-06	19.7065
3.96E-08	4.53529	7.36E-08	5.63771	1.33E-07	7.10868	2.89E-07	9.30358	7.14E-07	12.96069	5.66E-06	19.90037
3.92E-08	4.55513	7.40E-08	5.66233	1.35E-07	7.14393	3.02E-07	9.35758	7.29E-07	13.05801	5.74E-06	20.08676
4.00E-08	4.57506	7.42E-08	5.68794	1.37E-07	7.17975	2.91E-07	9.41453	7.47E-07	13.15719	6.50E-06	20.2972
4.17E-08	4.5949	7.55E-08	5.71347	1.38E-07	7.21571	2.86E-07	9.46969	7.64E-07	13.25745		
4.15E-08	4.61495	7.59E-08	5.73901	1.41E-07	7.25155	2.90E-07	9.52649	7.83E-07	13.35752		

Table A-4. Crack Growth Rate Data for the Alternating Immersion Salt-water Tests on the Normalized A516 Steel

Crack Length (inch)	Cycle Count	ΔK (ksi in ^{1/2})	da/dN (in/cycle)	Crack Length (inch)	Cycle Count	ΔK (ksi in ^{1/2})	da/dN (in/cycle)
0.467756	1032309	4.83E-07	8.10223	0.506578	1242857	2.22E-07	8.0566
0.467616	1032410	-1.94E-06	8.1083	0.507965	1248887	2.47E-07	8.05495
0.467364	1032511	6.93E-07	8.11114	0.50941	1254314	2.65E-07	8.05273
0.467756	1032612	1.74E-06	8.10644	0.51075	1259376	2.63E-07	8.05114
0.467714	1032713	9.58E-08	8.1122	0.512071	1264435	2.68E-07	8.04879
0.467897	1034076	1.98E-07	8.10868	0.513461	1269494	2.68E-07	8.04689
0.468917	1038799	2.05E-07	8.10784	0.514844	1274794	2.61E-07	8.04499
0.470341	1046014	1.96E-07	8.10654	0.51623	1280094	2.25E-07	8.04254
0.471186	1053779	2.01E-07	8.10453	0.517395	1286117	2.21E-07	8.04077
0.473293	1060709	2.02E-07	8.10286	0.518948	1292380	2.43E-07	8.03849
0.474543	1067079	2.11E-07	8.1009	0.520323	1298162	2.4E-07	8.03667
0.476012	1073565	2.12E-07	8.09929	0.521722	1303944	2.42E-07	8.03478
0.477336	1080266	2.23E-07	8.09761	0.523124	1309726	2.36E-07	8.03255
0.478901	1086531	2.48E-07	8.09576	0.52456	1315990	2.23E-07	8.03059
0.48026	1092077	1.78E-07	8.09344	0.525967	1322494	2.21E-07	8.02856
0.481513	1101234	1.22E-07	8.09162	0.527274	1328276	2.35E-07	8.02673
0.482919	1113829	1.24E-07	8.08941	0.528574	1333576	2.42E-07	8.02475
0.484414	1124683	1.5E-07	8.08768	0.53001	1339599	2.26E-07	8.02288
0.485841	1133348	1.67E-07	8.08629	0.531408	1346103	2.24E-07	8.02069
0.487188	1141260	1.79E-07	8.08419	0.532818	1352126	2.3E-07	8.01849
0.488611	1148796	1.66E-07	8.08215	0.53423	1358390	2.22E-07	8.01662
0.489884	1157461	1.51E-07	8.08027	0.535655	1364894	2.17E-07	8.01446
0.491292	1166504	1.68E-07	8.07824	0.537052	1371399	2.14E-07	8.01272
0.49274	1174416	1.89E-07	8.07648	0.538382	1377662	2.22E-07	8.01051
0.494133	1181574	1.96E-07	8.07442	0.539784	1383685	2.38E-07	8.00904
0.495461	1188282	1.98E-07	8.07243	0.541188	1389467	2.38E-07	8.00665
0.496839	1195218	1.98E-07	8.07023	0.542535	1395249	2.33E-07	8.00503
0.498268	1202454	1.98E-07	8.06829	0.543934	1401271	2.35E-07	8.00291
0.499643	1209388	1.99E-07	8.06625	0.545315	1407053	2.4E-07	8.00086
0.500966	1216021	2E-07	8.06448	0.546707	1412835	2.35E-07	7.99903
0.50236	1222956	2.02E-07	8.06232	0.548036	1418617	2.91E-07	8.00205
0.50377	1229891	2.11E-07	8.06047	0.549856	1423638	1.19E-06	8.00466
0.505217	1236525	2.17E-07	8.05849	0.556248	1425507	3.15E-06	7.99299

Table A-5. Crack Growth Rate Data for the Full Immersion Salt-water Tests on the Normalized A516 Steel

ΔK (ksi in ^{1/2})	da/dN (in/cycle)
12	2.37E-07
12	3.75E-07
12	3.11E-07
12	2.52E-07

Table A-6. Fracture Test Data for the Location A of the Pulse MIG Welded A516 Steel

1WA		2WA		3WA		6WA		5WA		4WA	
Δa	J1820	Δa	J1820								
inch	lbf/in	inch	lbf/in								
0.0030	260.76	0.0031	256.50	0.0028	341.50	0.0012	338.49	-0.000994	301.8181	-0.001335	338.1222
0.0038	327.76	0.0019	327.94	0.0006	427.76	0.0011	420.27	-0.002214	371.7014	0.000391	410.044
0.0031	403.01	0.0013	403.64	-0.0010	509.16	0.0007	503.62	-0.0005	443.8547	-2.31E-05	491.6038
0.0015	480.92	-0.0002	483.81	0.0022	594.17	0.0022	585.84	-0.000609	515.1351	0.001281	566.4342
0.0023	554.61	0.0018	558.26	0.0014	681.49	-0.0003	675.66	0.000764	586.609	0.000797	640.6708
0.0010	635.99	0.0007	639.25	0.0007	777.17	0.0004	769.39	-0.001067	665.0536	0.000442	720.0327
0.0013	714.47	0.0019	716.85	0.0009	866.34	0.0000	859.23	0.004646	735.81	0.002158	798.1188
0.0009	799.36	0.0002	803.39	0.0040	946.36	0.0004	951.51	0.001616	814.0023	0.003199	874.7272
0.0000	883.25	0.0016	883.19	0.0043	1033.98	0.0030	1040.35	0.00285	891.9021	-0.00143	977.2152
0.0025	963.87	0.0023	966.47	0.0040	1121.36	0.0058	1129.85	0.002513	971.2241	0.007012	1047
0.0026	1044.21	0.0006	1055.04	0.0071	1205.58	0.0039	1223.34	0.007041	1043.716	0.006182	1128.847
0.0039	1126.48	0.0033	1135.02	0.0093	1295.99	0.0052	1315.93	0.006258	1121.248	0.00784	1209.203
0.0041	1213.66	0.0041	1217.71	0.0092	1386.72	0.0059	1406.48	0.006192	1198.751	0.008864	1289.205
0.0040	1295.53	0.0028	1305.65	0.0074	1485.31	0.0078	1499.34	0.007594	1276.542	0.008133	1371.96
0.0042	1383.81	0.0015	1394.10	0.0123	1567.40	0.0090	1588.26	0.007389	1354.911	0.008249	1459.208
0.0051	1462.51	0.0030	1480.85	0.0098	1672.25	0.0110	1682.49	0.006771	1438.273	0.011792	1542.361
0.0053	1549.45	0.0047	1564.51	0.0141	1762.05	0.0101	1777.53	0.009008	1517.064	0.015576	1622.212
0.0067	1638.14	0.0051	1653.85	0.0131	1861.29	0.0135	1870.80	0.016895	1589.35	0.015009	1707.993
0.0084	1721.63	0.0052	1743.84	0.0172	1947.31	0.0148	1961.72	0.01288	1677.303	0.015025	1793.55
0.0089	1808.09	0.0084	1831.77	0.0166	2040.71	0.0186	2050.25	0.011387	1761.776	0.020782	1867.575
0.0110	1892.34	0.0108	1921.16	0.0204	2129.65	0.0165	2151.64	0.013051	1842.638	0.020973	1951.778
0.0082	1985.12	0.0148	2003.90	0.0214	2223.63	0.0205	2242.64	0.018305	1920.322	0.02458	2030.852
0.0132	2067.38	0.0161	2093.02	0.0231	2316.70	0.0187	2347.13	0.020043	1999.048	0.023107	2121.787
0.0111	2160.15	0.0175	2183.54	0.0241	2413.76	0.0225	2439.89	0.02003	2081.813	0.026053	2202.644
0.0142	2244.09	0.0178	2281.18	0.0259	2510.57	0.0228	2539.86	0.020108	2165.546	0.025903	2291.361
0.0153	2330.96	0.0220	2366.82	0.0300	2600.03	0.0251	2634.12	0.023315	2243.188	0.032183	2363.62
0.0189	2415.17	0.0251	2452.29	0.0321	2695.76	0.0277	2731.09	0.02942	2314.979	0.03219	2449.244
0.0206	2504.81	0.0276	2539.36	0.0345	2790.53	0.0281	2837.41	0.031587	2394.254	0.03285	2535.193
0.0205	2597.77	0.0277	2635.83	0.0388	2879.61	0.0316	2931.91	0.027877	2487.506	0.037746	2701.329
0.0253	2676.21	0.0307	2722.77	0.0421	2971.21	0.0368	3026.85	0.030941	2565.522	0.039743	2783.611
0.0257	2767.07	0.0329	2817.20	0.0444	3062.11	0.0393	3121.64	0.034242	2643.402	0.04305	2865.716
0.0303	2852.81	0.0369	2903.30	0.0508	3149.86	0.0424	3221.97	0.036221	2725.265	0.043973	2953.963
0.0322	2938.20	0.0423	2982.77	0.0529	3242.44	0.0456	3319.70	0.040203	2801.149	0.048113	3031.242
0.0373	3016.45	0.0427	3081.69	0.0578	3330.50	0.0520	3409.77	0.042653	2882.25	0.051948	3109.921
0.0404	3106.74	0.0483	3157.04	0.0622	3426.28	0.0608	3490.91	0.045315	2960.849	0.054789	3191.246
0.0443	3191.57	0.0500	3248.47	0.0676	3514.56	0.0676	3580.76	0.049309	3038.911	0.060778	3262.378
0.0513	3267.31	0.0502	3350.69	0.0724	3599.18	0.0731	3675.73	0.055378	3110.672	0.065455	3336.915
0.0556	3350.68	0.0568	3427.33	0.4845	5515.69	0.0782	3760.63	0.062135	3179.389	0.066838	3433.447
0.0620	3434.71	0.0596	3516.01	0.4866	5578.87	0.0863	3839.23	0.06416	3267.019	0.076129	3502.188
0.0710	3505.30	0.0645	3597.16	0.4994	5595.21	0.0970	3912.88	0.073783	3327.459		
0.0802	3576.56	0.0709	3677.98	0.5052	5642.97	0.1418	3992.30	0.081342	3391.608		
0.1698	4040.52	0.0776	3751.86			0.1531	4048.10	0.086446	3461.682		
0.1768	4116.51	0.3189	5202.66			0.1602	4129.18				
0.1833	4186.10	0.3255	5270.01			0.1728	4185.03				

Table A-7. Fracture Test Data for the Location B of the Pulse MIG Welded A516 Steel

5WB		2WB		7WB		3WB		4WB		6WB	
Δa	J1820										
inch	lbf/in										
0.000427	339.2228	0.000306	289.0262	-4.07E-05	258.8937	0.002413	188.0135	0.001813	328.6544	0.002582	247.9544
8.39E-05	412.863	0.001606	355.5158	-0.000613	324.3135	0.002467	247.1096	0.001772	400.9227	0.001663	310.4493
0.000152	486.666	0.001794	428.6952	0.000632	390.5028	0.000755	308.0975	0.001998	474.416	0.00068	380.1634
0.000608	562.2147	0.002416	508.6322	0.001018	459.4758	0.000125	374.8128	0.000794	549.9891	0.003579	446.1654
-0.000888	640.6392	0.003043	581.6824	-7.2E-05	539.6904	0.001999	447.9086	0.00299	629.3292	0.003252	515.6492
0.002657	715.5604	0.003254	655.8414	0.005152	607.5174	0.00054	516.7962	0.005808	704.5923	0.002161	591.9564
0.003556	793.9114	0.002644	735.7219	0.002883	682.9087	0.00092	592.0143	0.003249	784.6449	0.002674	666.7694
0.001676	874.2715	0.00542	812.4869	0.001534	761.6768	0.003852	661.0301	0.002298	870.097	0.004058	741.6642
0.003575	952.5905	0.00247	890.1779	0.006058	833.737	0.007166	808.4735	0.006201	947.9458	0.002981	825.4413
0.002924	1034.832	0.004345	967.2903	0.006914	908.2129	0.006756	888.8132	0.004112	1031.191	0.005475	901.2552
8.64E-05	1125.723	0.000796	1054.817	0.006008	986.9764	0.008483	963.694	0.01198	1116.553	0.005561	980.0563
0.007581	1200.928	0.005197	1128.213	0.00904	1063.547	0.007521	1042.332	0.010031	1199.229	0.004737	1060.878
0.010373	1280.094	0.003693	1208.418	0.011709	1141.41	0.00983	1117.392	0.010079	1281.216	0.006889	1142.338
0.011042	1361.939	0.005346	1289.059	0.008167	1232.235	0.006748	1207.008	0.010255	1364.873	0.009595	1220.672
0.013259	1444.099	0.007008	1369.954	0.014598	1303	0.01177	1283.151	0.011567	1448.447	0.010778	1298.973
0.014561	1526.922	0.009078	1450.12	0.01828	1378.986	0.007977	1374.483	0.014074	1532.033	0.010514	1384.316
0.017582	1605.21	0.01296	1526.692	0.017839	1460.691	0.014481	1446.675	0.013828	1618.231	0.014804	1460.32
0.01862	1688.46	0.016487	1604.282	0.018522	1545.342	0.017357	1523.546	0.015048	1702.36	0.017668	1538.547
0.01996	1771.279	0.018191	1684.721	0.022191	1620.885	0.018448	1602.942	0.016909	1788.212	0.019427	1618.696
0.022586	1853.502	0.020909	1763.878	0.023588	1700.533	0.01872	1687.08	0.017634	1873.188	0.021427	1698.916
0.022963	1939.421	0.021773	1846.474	0.024421	1782.446	0.024269	1762.684	0.01975	1958.31	0.023368	1779.392
0.025786	2019.421	0.024703	1927.046	0.027275	1861.707	0.024755	1844.056	0.021104	2043.058	0.025975	1863.448
0.027491	2101.909	0.027903	2009.552	0.029905	1940.074	0.025491	1926.238	0.024881	2122.585	0.029783	1939.837
0.025989	2194.543	0.028838	2092.324	0.029979	2027.536	0.029888	2002.587	0.024666	2212.856	0.030238	2024.502
0.032884	2266.33	0.029314	2177.708	0.034235	2103.847	0.031265	2084.27	0.029961	2290.331	0.032025	2108.644
0.034329	2350.812	0.032579	2257.014	0.034924	2188.508	0.033428	2165.701	0.029684	2379.096	0.032043	2194.414
0.034904	2437.145	0.034627	2337.191			0.036907	2243.135	0.030593	2465.621	0.03452	2273.578
0.034396	2524.97	0.037278	2416.708			0.039843	2323.839	0.033465	2548.282	0.035281	2358.126
0.036793	2607.729	0.039273	2498.838			0.039358	2414.918	0.033105	2638.705	0.035907	2442.574
0.038512	2690.008	0.04362	2576.124			0.042252	2497.809	0.036287	2720.565	0.03778	2525.71
0.040288	2773.557	0.042291	2667.925			0.04448	2581.325	0.038488	2804.592	0.039115	2608.688
0.040802	2862.064	0.045812	2747.621			0.046948	2660.847	0.040349	2890.344	0.040765	2692.069
0.041766	2949.807	0.047093	2833.097			0.046767	2749.592	0.041435	2977.193	0.043044	2774.44
0.043636	3033.539	0.066695	3408.152			0.050226	2827.252	0.044662	3059.913	0.042807	2864.851
0.045238	3118.458	0.090918	3963.055			0.053325	2905.262	0.047838	3141.772	0.043539	2950.97
						0.057599	2981.033	0.048369	3231.885	0.047625	3029.357
						0.056386	3070.955	0.047405	3327.721	0.047737	3118.662
						0.056826	3161.139				
						0.060298	3238.421				
						0.060524	3328.225				
						0.063594	3408.13				
						0.063931	3497.758				

Table A-8. Fracture Test Data for the Location C of the Pulse MIG Welded A516 Steel

1WC		1WC-3		3WC		5WC		4WC		2WC	
Δa	J1820										
inch	lbf/in										
0.000662	283.8527	0.000483	241.8879	0.001774	166.4263	0.003852	209.4329	0.00198	331.5204	0.003143	296.6563
0.001065	351.3054	0.00124	301.7477	0.001588	219.1855	0.002315	264.7365	3.05E-05	401.0797	0.001176	365.7214
0.000538	419.1686	0.000494	364.1298	0.001516	275.2681	0.003486	328.911	0.001452	475.4286	0.001428	438.6967
9.76E-05	489.2317	0.000356	429.9885	0.001674	333.0505	0.001396	388.9261	-0.000679	554.2714	0.004583	510.6515
0.000444	561.1784	1.11E-05	497.915	0.000627	395.4677	0.002101	453.0442	0.000588	625.8065	-0.001643	588.5044
0.000548	632.494	0.001219	565.672	0.001752	457.6957	0.000478	522.3094	0.001827	699.1954	0.000276	664.8997
0.00244	704.8689	0.001069	635.6243	0.000648	526.3587	-0.002741	595.6138	0.0032	775.405	0.000655	738.1019
0.000632	779.6584	0.001838	705.4134	0.0013	593.1528	0.000872	662.6719	9.91E-05	852.2036	0.000296	815.4935
0.00445	850.187	0.001537	775.3374	0.002469	660.7202	-0.002685	734.5225	-0.000133	930.5032	-0.000992	899.958
0.003308	925.9492	-1.76E-05	850.9999	0.001316	731.5189	0.005482	801.7922	0.004786	1005.702	0.001435	977.0018
0.004648	998.9233	0.001537	922.2534	0.002027	800.3353	0.00454	872.173	0.002802	1087.643	-0.004661	1062.67
0.002028	1086.037	0.001377	995.321	0.002243	874.1163	0.002864	946.9847	0.00545	1166.849	0.007845	1128.921
0.007459	1154.815	0.00345	1067.191	0.004031	943.751	0.001764	1018.839	0.006034	1241.743	0.003878	1214.11
0.00704	1232.631	0.003155	1140.856	0.003856	1018.882	0.003516	1094.935	0.005111	1322.901	-0.002291	1311.06
0.006745	1311.256	0.002368	1218.622	0.004415	1093.021	0.002524	1178.372	0.006532	1399.832	0.001511	1396.156
0.007905	1388.95	0.003481	1296.113	0.005233	1167.784	0.005628	1250.053	0.009273	1478.969	0.012366	1465.083
0.009579	1464.719	0.004277	1369.712	0.005178	1243.85	0.002269	1334.073	0.008988	1560.901	0.014378	1546.439
0.010722	1544.592	0.00449	1448.844	0.006057	1322.91	0.00591	1406.244	0.012727	1637.889	0.011067	1633.7
0.012597	1622.224	0.004696	1526.318	0.009371	1395.059	0.007706	1479.319	0.013493	1721.215	0.003671	1734.193
0.014428	1699.922	0.006003	1601.288	0.010231	1470.112	0.004749	1569.96	0.01445	1806.98	0.013056	1802.049
0.016498	1775.814	0.007708	1676.057	0.009368	1548.622	0.010858	1641.528	0.017876	1887.935	0.011674	1886.754
0.014985	1860.874	0.006803	1757.331	0.010435	1624.252	0.009197	1722.549	0.0196	1968.805	0.016138	1965.757
0.017661	1938.977	0.008047	1834.625	0.010958	1704.848	0.014181	1790.537	0.023281	2042.129	0.014552	2049.224
0.020526	2015.069	0.011278	1907.209	0.014109	1778.466	0.014951	1869.988	0.023289	2123.937	0.018557	2124.344
0.023559	2091.701	0.01082	1987.137	0.014209	1857.173	0.017251	1944.982	0.022696	2206.554	0.021958	2206.144
0.022584	2174.964	0.011805	2064.307	0.016173	1935.183	0.018928	2019.308	0.028492	2283.026	0.021236	2288.843
0.027791	2247.994	0.015334	2138.31	0.018326	2009.479	0.020436	2102.564	0.031559	2362.106	0.024325	2363.476
0.028412	2328.065	0.019073	2211.366	0.020361	2085.153	0.021339	2185.856	0.034545	2436.921	0.023452	2454.611
0.029386	2409.321	0.018701	2291.781	0.021493	2164.443	0.023312	2260.13	0.034833	2519.559	0.0274	2528.865
0.032479	2486.279	0.018945	2371.582	0.022831	2241.512	0.027655	2331.935	0.038356	2599.221	0.027902	2616.921
0.032719	2570.763	0.019795	2456.313	0.023432	2325.4	0.027026	2416.84	0.044724	2671.269	0.030082	2699.077
		0.023516	2528.25	0.028988	2393.54	0.029116	2496.197	0.04575	2753.446	0.039745	2937.931
		0.026648	2602.843	0.030621	2470.78	0.027788	2583.27			0.037801	3027.558
		0.028938	2678.12	0.035246	2542.553	0.036727	2646.943			0.045097	3092.767
		0.030234	2754.563	0.038557	2616.601	0.035213	2729.233			0.050885	3160.232
		0.03385	2827.203	0.042153	2690.289	0.036566	2814.836			0.056385	3232.54
		0.036004	2904.056	0.046695	2761.476	0.039003	2894.909			0.060076	3308.866
		0.041011	2975.912	0.051988	2829.552					0.059702	3397.62
		0.046308	3045.559	0.053484	2907.829					0.065015	3466.054
		0.048206	3122.718	0.058586	2975.892					0.066904	3547.105
				0.061179	3050.569					0.078188	3601.37
				0.06425	3125.038						
				0.067378	3200.625						
				0.076365	3257.114						
				0.0789	3333.902						
				0.083139	3404.739						

Table A-9. Fracture Test Data for the HAZ of the Flux-cored Welded A516 Steel

A1			B1			C1		
Δa	Je	J1820	Δa	J1820	Je	Δa	Je	J1820
inch	lbf/in	lbf/in	inch	lbf/in	lbf/in	inch	lbf/in	lbf/in
0.0024	160.76	170.60	0.0019	204.28	184.03	0.0019	246.05	206.73
0.0027	172.46	246.23	0.0027	531.51	210.97	0.0026	333.83	214.02
0.0023	180.93	324.75	0.0067	1163.82	255.62	0.0039	427.16	223.03
0.0024	187.38	407.02	0.0140	1840.18	283.29	0.0035	520.68	227.58
0.0019	194.95	491.72	0.0726	3673.40	313.64	0.0042	613.72	234.36
0.0031	199.33	571.49	0.0770	3768.08	322.24	0.0052	710.79	240.85
0.0031	208.24	658.67	0.0836	3856.88	326.45	0.0052	804.88	245.58
0.0045	215.62	748.10	0.0904	3950.35	323.84	0.0058	902.16	251.84
0.0041	220.53	839.15	0.1007	4021.89	325.45	0.0077	997.95	257.56
0.0053	227.80	931.45				0.0081	1095.15	262.56
0.0062	232.57	1023.42				0.0077	1197.74	265.82
0.0059	237.47	1116.53				0.0092	1297.47	271.57
0.0080	244.16	1211.42				0.0104	1397.15	276.34
0.0075	247.84	1311.17				0.0107	1496.87	279.36
0.0094	253.81	1408.28				0.0115	1595.45	283.23
0.0096	257.84	1513.21				0.0127	1691.78	287.88
0.0111	262.83	1609.41				0.0145	1800.96	293.64
0.0117	265.11	1715.13				0.0146	1902.17	295.55
0.0139	272.90	1819.34				0.0151	2006.88	298.85
0.0140	275.65	1920.51				0.0164	2105.30	301.74
0.0166	280.58	2017.87				0.0187	2204.47	305.78
0.0172	282.83	2124.40				0.0190	2308.71	308.42
0.0203	287.85	2222.00				0.0198	2419.58	310.68
0.0221	290.20	2326.29				0.0234	2518.36	315.34
0.0261	295.58	2425.12				0.0241	2627.26	316.59
0.0285	298.27	2520.59				0.0258	2729.00	318.61
0.0344	304.55	2609.16				0.0286	2829.76	321.73
0.0354	305.58	2724.29				0.0304	2934.40	322.88
0.0379	308.42	2824.84				0.0328	3038.38	324.57
0.0395	309.74	2931.80				0.0370	3131.33	326.44
0.0441	312.73	3024.83				0.0406	3235.17	327.13
0.0473	315.30	3124.48				0.0462	3326.83	329.29
0.0498	316.90	3232.15				0.0491	3427.92	330.49
0.0519	317.18	3335.83				0.0541	3534.00	330.43
0.0529	316.99	3445.09				0.0576	3639.72	329.83
0.0571	317.74	3537.49				0.0631	3732.01	332.57
0.0612	318.59	3631.14				0.0676	3836.76	330.38
0.0662	319.78	3725.12				0.0746	3916.15	327.60
0.0699	319.55	3823.13						
0.0771	319.95	3904.62						
0.0835	319.00	3991.86						

Table A-10. Fracture Test Data for the Weld of the Flux-cored Welded A516 Steel

A2			B2			C2		
Δa	J1820	Je	Δa	J1820	Je	Δa	J1820	Je
inch	lbf/in	lbf/in	inch	lbf/in	lbf/in	inch	lbf/in	lbf/in
0.0030	165.72	162.79	0.0034	204.29	198.59	0.0044	242.35	233.77
0.0015	230.57	195.69	0.0035	279.85	223.85	0.0040	327.57	258.66
0.0014	303.76	224.95	0.0045	370.71	241.39	0.0045	420.91	270.82
0.0017	387.37	247.73	0.0054	465.65	253.06	0.0055	515.02	280.74
0.0041	479.48	259.80	0.0075	563.19	263.23	0.0053	622.71	287.25
0.0045	579.81	269.75	0.0083	664.65	272.29	0.0098	723.21	296.47
0.0058	679.48	281.23	0.0116	765.74	281.98	0.0095	830.48	302.07
0.0068	776.69	288.62	0.0139	870.58	290.10	0.0121	938.69	308.46
0.0092	882.08	299.10	0.0168	972.34	297.20	0.0153	1040.59	315.15
0.0109	988.67	307.14	0.0214	1070.05	305.12	0.0171	1155.19	320.33
0.0108	1111.65	315.56	0.0235	1182.47	311.17	0.0203	1264.07	326.01
0.0144	1217.40	322.12	0.0276	1285.09	317.84	0.0230	1374.91	329.65
0.0167	1325.38	326.82	0.0302	1396.74	323.39	0.0243	1485.65	334.21
0.0207	1435.95	334.08	0.0336	1508.99	327.51	0.0286	1599.87	340.66
0.0227	1550.44	338.35	0.0382	1617.31	333.27	0.0295	1705.95	342.42
0.0277	1666.20	342.91	0.0408	1726.25	335.81	0.0325	1809.45	346.95
0.0327	1777.24	349.32	0.0461	1829.87	341.48	0.0348	1921.10	351.11
0.0391	1889.94	349.40	0.0479	1942.22	342.96	0.0385	2043.33	350.92
0.0440	2011.39	355.07	0.0527	2058.60	348.26	0.0444	2144.08	352.61
0.0491	2119.18	357.94	0.0563	2168.28	350.93	0.0512	2251.47	356.81
0.0549	2221.62	357.49	0.0617	2281.21	353.24	0.0583	2357.52	361.81
0.0607	2333.02	363.78	0.0652	2386.38	354.07	0.0625	2478.77	361.01
0.0663	2447.20	366.38	0.0709	2489.63	357.25	0.0709	2586.36	361.28
0.0708	2559.46	368.80	0.0759	2602.59	357.25	0.0769	2691.97	361.84
0.0741	2668.44	370.61	0.0818	2705.73	362.19	0.0814	2809.65	360.86
0.0786	2769.83	372.15	0.0857	2815.64	361.87	0.0900	2908.47	361.51
0.0832	2878.12	377.26	0.0915	2918.70	360.79	0.1021	2987.81	352.48
0.0878	3000.43	378.26	0.0971	3022.99	367.72	0.1125	3061.42	348.71
0.0981	3095.05	379.64	0.1021	3126.90	364.95	0.1270	3126.51	354.26
0.1102	3172.83	381.09	0.1071	3231.93	367.11	0.1377	3203.74	353.04
0.1217	3255.80	372.89	0.1138	3328.69	365.93	0.1490	3273.97	350.49
0.1309	3332.23	375.87	0.1186	3429.73	365.79	0.1597	3340.53	350.43
			0.1230	3540.82	372.64	0.1675	3407.08	349.13
			0.1310	3616.86	364.14			

Table A-11. Fracture Test Data for the Parent 0° Location of the Flux-cored Welded A516 Steel

A3			B3			C3		
Δa	J1820	Je	Δa	J1820	Je	Δa	J1820	Je
inch	lbf/in	lbf/in	inch	lbf/in	lbf/in	inch	lbf/in	lbf/in
0.0047	205.39	165.35	0.0039	202.47	176.59	0.0021	227.21	185.78
0.0043	289.38	170.36	0.0047	280.11	181.21	0.0027	310.25	189.22
0.0039	375.58	175.25	0.0044	363.70	184.63	0.0037	392.48	192.64
0.0046	452.73	179.87	0.0044	443.37	188.13	0.0040	478.86	195.63
0.0041	536.64	184.13	0.0038	531.91	190.92	0.0044	557.82	198.03
0.0057	621.28	189.41	0.0051	616.91	194.20	0.0063	641.78	202.13
0.0041	706.24	192.54	0.0063	702.66	198.06	0.0068	724.77	204.77
0.0066	791.35	198.11	0.0066	786.16	200.40	0.0059	811.14	207.01
0.0058	877.72	201.43	0.0061	873.64	202.67	0.0070	900.39	210.84
0.0075	966.62	206.15	0.0069	954.95	205.38	0.0100	986.46	215.46
0.0073	1055.30	209.09	0.0088	1043.35	209.91	0.0099	1072.97	217.95
0.0092	1139.87	214.21	0.0107	1132.36	214.26	0.0096	1161.19	219.81
0.0101	1232.13	218.01	0.0100	1223.39	215.72	0.0100	1244.34	222.53
0.0096	1328.87	221.01	0.0104	1314.13	218.39	0.0121	1331.43	226.25
0.0124	1418.97	225.25	0.0120	1397.28	221.37	0.0132	1419.89	230.00
0.0119	1513.84	227.93	0.0141	1483.80	225.10	0.0134	1511.02	232.43
0.0148	1601.31	232.54	0.0138	1573.96	227.55	0.0138	1597.71	234.18
0.0142	1699.66	234.35	0.0152	1662.85	230.30	0.0150	1691.88	238.12
0.0173	1783.70	239.12	0.0169	1747.74	233.17	0.0170	1776.90	241.59
0.0167	1877.38	240.74	0.0184	1833.86	236.34	0.0164	1876.12	243.68
0.0201	1961.95	245.33	0.0197	1920.88	239.37	0.0178	1961.82	246.07
0.0194	2062.01	246.52	0.0197	2013.66	241.02	0.0197	2049.44	249.81
0.0231	2142.15	251.13	0.0221	2102.02	244.79	0.0215	2139.18	252.84
0.0228	2237.82	253.02	0.0238	2190.69	248.26	0.0212	2235.67	254.37
0.0257	2328.38	257.22	0.0240	2287.68	249.87	0.0227	2318.14	257.02
0.0260	2425.93	259.12	0.0254	2379.67	252.77	0.0250	2406.01	260.53
0.0282	2526.43	262.62	0.0282	2460.18	256.40	0.0246	2504.86	262.44
0.0296	2621.23	264.94	0.0287	2555.43	257.93	0.0262	2599.16	265.25
0.0304	2718.78	266.92	0.0293	2647.19	260.02	0.0267	2693.25	266.79
0.0334	2806.85	270.98	0.0323	2736.64	263.51	0.0292	2778.68	270.67
0.0342	2902.76	271.72	0.0345	2825.05	265.79	0.0310	2866.77	272.83
0.0374	2989.89	275.61	0.0361	2917.70	267.46	0.0321	2958.98	274.86
0.0374	3092.21	276.78	0.0366	3016.08	268.98	0.0320	3056.72	275.91
0.0414	3172.30	281.17	0.0395	3100.46	272.19	0.0338	3144.82	278.53
0.0409	3274.93	281.61	0.0399	3195.34	273.35	0.0357	3233.98	281.26
0.0446	3365.34	286.11	0.0415	3289.31	275.38	0.0370	3325.04	283.76
0.0456	3473.38	286.95	0.0445	3370.95	278.35	0.0377	3423.39	285.31
0.0485	3563.13	288.95	0.0455	3472.60	279.97			
			0.0471	3561.67	282.06			
			0.0501	3650.06	285.31			

Table A-12. Fracture Test Data for the Parent 90° Location of the Flux-cored Welded A516 Steel

A4			B4			C4		
Δa	J1820	Je	Δa	J1820	Je	Δa	J1820	Je
inch	lbf/in	lbf/in	inch	lbf/in	lbf/in	inch	lbf/in	lbf/in
0.0038	126.35	118.81	0.0012	128.49	120.32	0.0039	155.80	138.41
0.0036	188.55	128.72	0.0024	198.07	131.01	0.0035	228.46	141.77
0.0044	255.62	136.81	0.0023	275.85	137.65	0.0047	302.80	146.69
0.0028	327.23	141.03	0.0029	349.89	142.11	0.0039	377.63	150.20
0.0040	403.44	145.93	0.0035	428.71	146.05	0.0031	457.22	153.14
0.0034	475.72	148.99	0.0039	509.23	149.48	0.0041	531.60	157.29
0.0039	556.12	153.04	0.0042	591.85	153.13	0.0053	610.92	160.47
0.0042	635.95	156.57	0.0046	669.51	156.07	0.0044	690.72	163.02
0.0046	715.00	159.43	0.0063	744.92	159.93	0.0060	770.60	166.48
0.0060	790.58	162.74	0.0056	823.71	162.85	0.0072	843.27	168.47
0.0057	868.09	165.17	0.0073	903.13	166.67	0.0069	925.97	172.07
0.0064	945.40	168.37	0.0074	977.33	169.19	0.0083	1009.30	176.13
0.0081	1021.95	171.96	0.0086	1061.48	173.80	0.0079	1091.98	178.67
0.0072	1100.21	173.78	0.0085	1143.82	176.17	0.0100	1171.21	182.08
0.0091	1176.77	177.55	0.0092	1222.53	179.23	0.0101	1256.00	184.98
0.0088	1263.56	180.95	0.0104	1300.24	182.55	0.0118	1337.14	189.01
0.0106	1348.29	184.49	0.0105	1380.41	185.07	0.0130	1422.77	191.61
0.0108	1426.46	186.27	0.0113	1461.74	188.08	0.0144	1513.93	195.51
0.0127	1506.73	190.52	0.0122	1542.47	190.96	0.0149	1603.59	197.43
0.0124	1592.14	192.43	0.0123	1622.79	193.83	0.0165	1686.94	200.79
0.0140	1670.18	195.56	0.0145	1704.52	197.58	0.0181	1766.70	204.13
0.0146	1753.61	198.43	0.0146	1787.73	199.86	0.0175	1860.94	206.03
0.0161	1831.29	201.33	0.0144	1874.77	202.28	0.0207	1939.79	210.14
0.0167	1919.75	204.52	0.0165	1950.57	205.36	0.0217	2027.06	212.82
0.0184	2003.40	207.29	0.0179	2030.10	209.03	0.0211	2115.28	214.26
0.0194	2089.77	209.75	0.0180	2116.99	210.90	0.0243	2198.20	218.74
0.0218	2183.98	213.93	0.0179	2202.37	212.97	0.0251	2291.33	220.43
0.0230	2280.18	216.06	0.0207	2282.72	217.29	0.0274	2378.26	223.88
0.0227	2372.97	217.94	0.0206	2374.47	219.02	0.0291	2467.45	226.30
0.0258	2455.95	221.42	0.0217	2464.34	222.01	0.0307	2550.78	228.46
0.0259	2545.59	222.77	0.0236	2542.29	224.57	0.0315	2645.08	230.58
0.0283	2626.11	226.16	0.0241	2634.00	226.65	0.0344	2725.92	233.89
0.0285	2716.54	227.17	0.0256	2721.38	229.41	0.0352	2821.63	235.68
0.0313	2804.72	230.93	0.0272	2807.88	232.49	0.0369	2908.89	237.46
0.0319	2897.62	232.44	0.0276	2900.01	233.20	0.0394	2993.03	240.92
0.0343	2977.85	235.01	0.0311	2972.73	237.36	0.0409	3078.83	242.17
0.0358	3063.86	236.94	0.0325	3065.25	239.78	0.0424	3173.71	244.12
0.0382	3151.81	240.26	0.0328	3153.71	240.41	0.0447	3258.49	246.78
0.0391	3243.74	241.38	0.0357	3238.11	242.94	0.0464	3351.55	248.42
0.0418	3329.68	243.81	0.0384	3312.33	245.81	0.0488	3433.98	250.03
0.0430	3420.87	244.85	0.0363	3420.23	245.48	0.0520	3521.30	252.77
0.0459	3503.93	247.85	0.0398	3494.87	248.29	0.0540	3613.92	253.96
0.0487	3586.42	248.59	0.0418	3579.77	251.35			
			0.0443	3662.58	254.31			

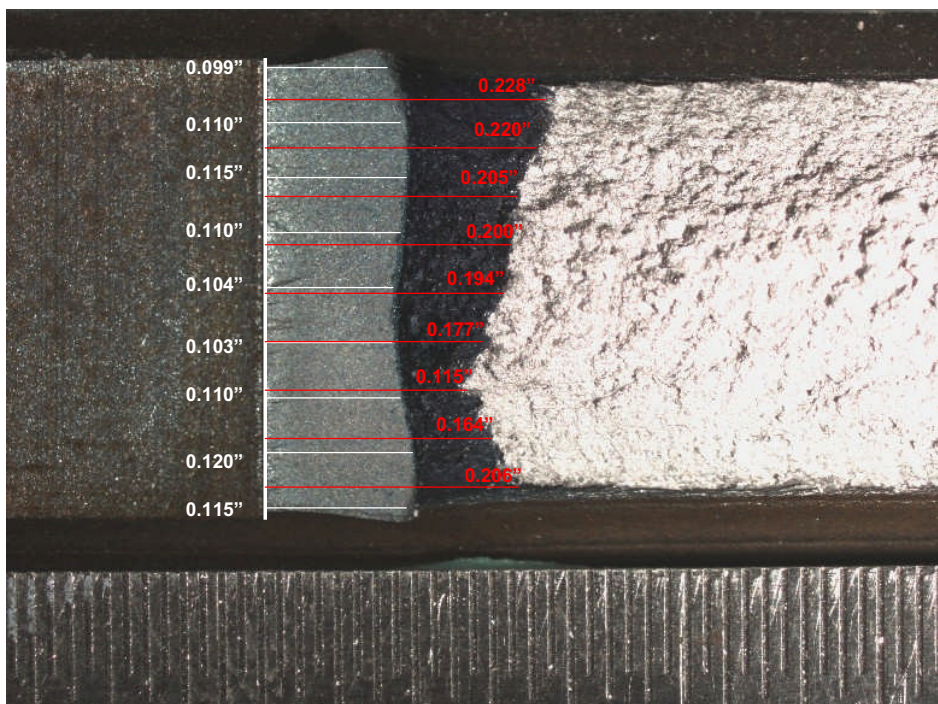


Figure A-1. Crack length measurements for specimen A1 (HAZ) of the flux-cored welded A516 steel

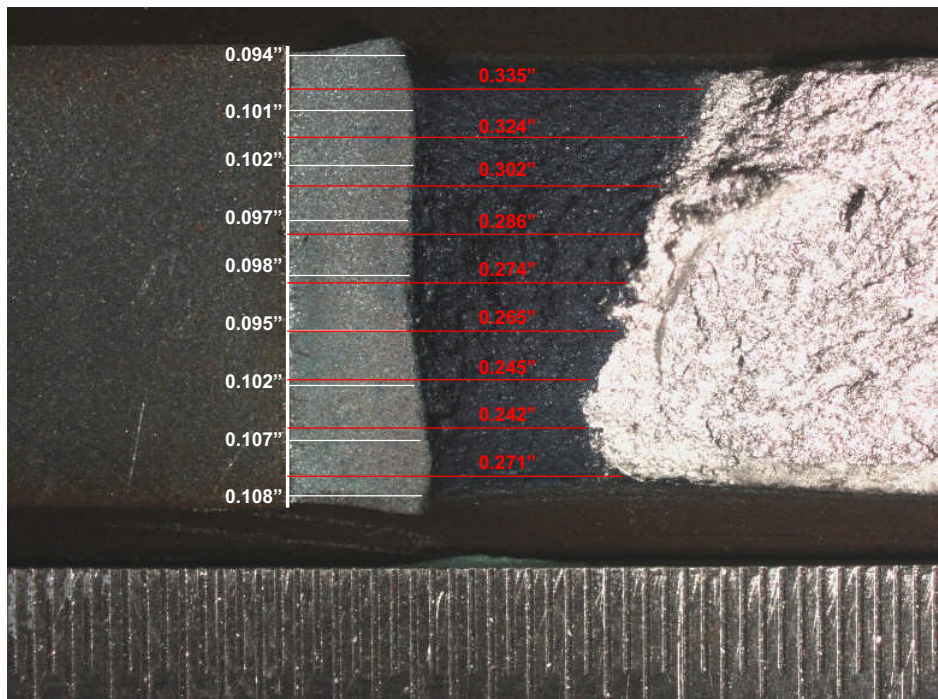


Figure A-2. Crack length measurements for specimen B1 (HAZ) of the flux-cored welded A516 steel



Figure A-3. Crack length measurements for specimen C1 (HAZ) of the flux-cored welded A516 steel

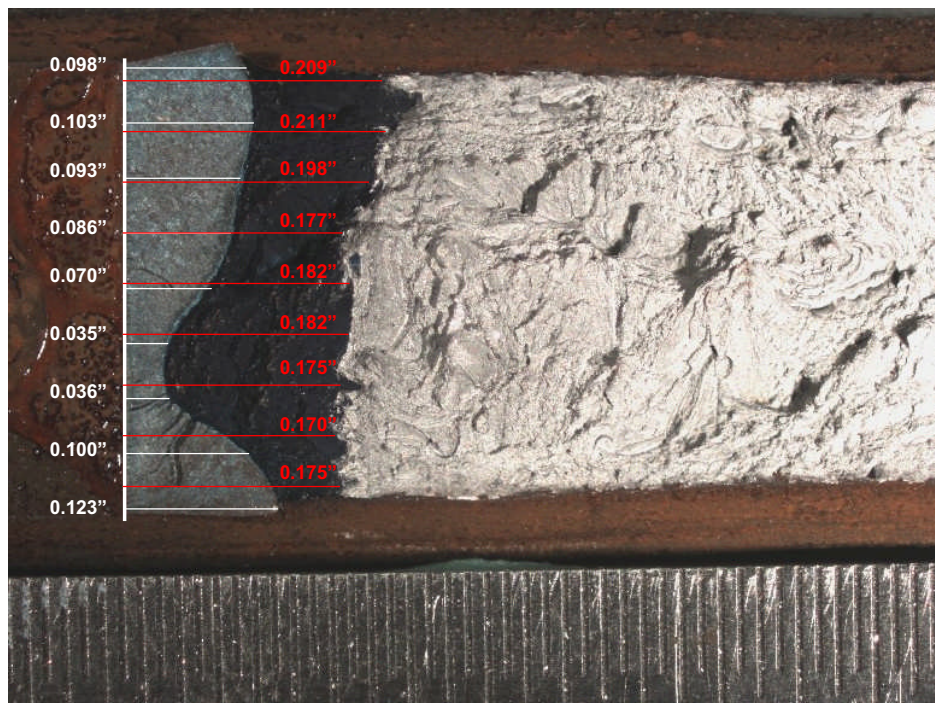


Figure A-4. Crack length measurements for specimen A2 (weld) of the flux-cored welded A516 steel

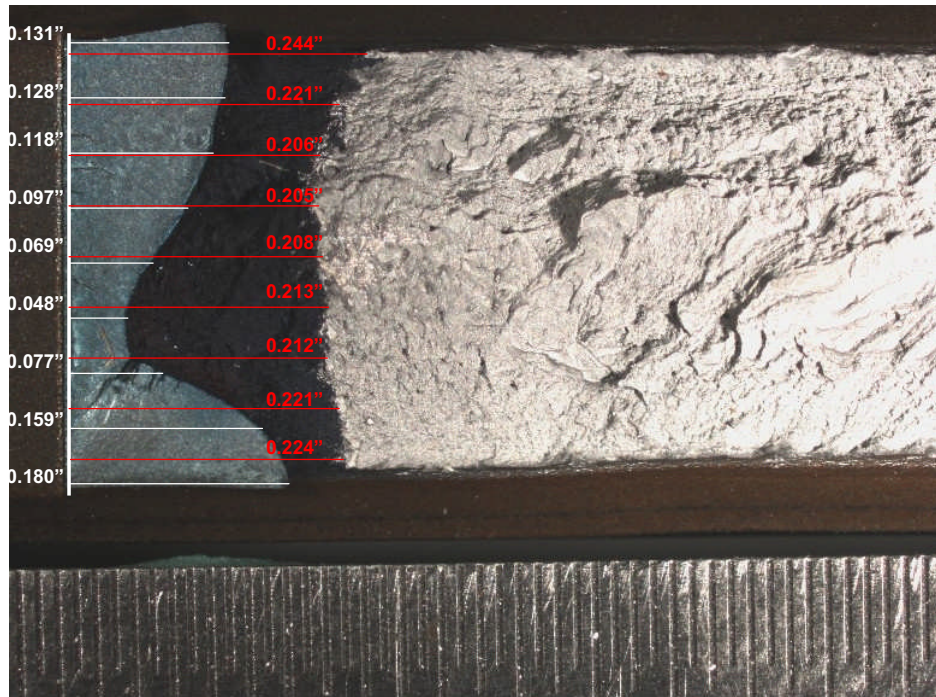


Figure A-5. Crack length measurements for specimen B2 (weld) of the flux-cored welded A516 steel

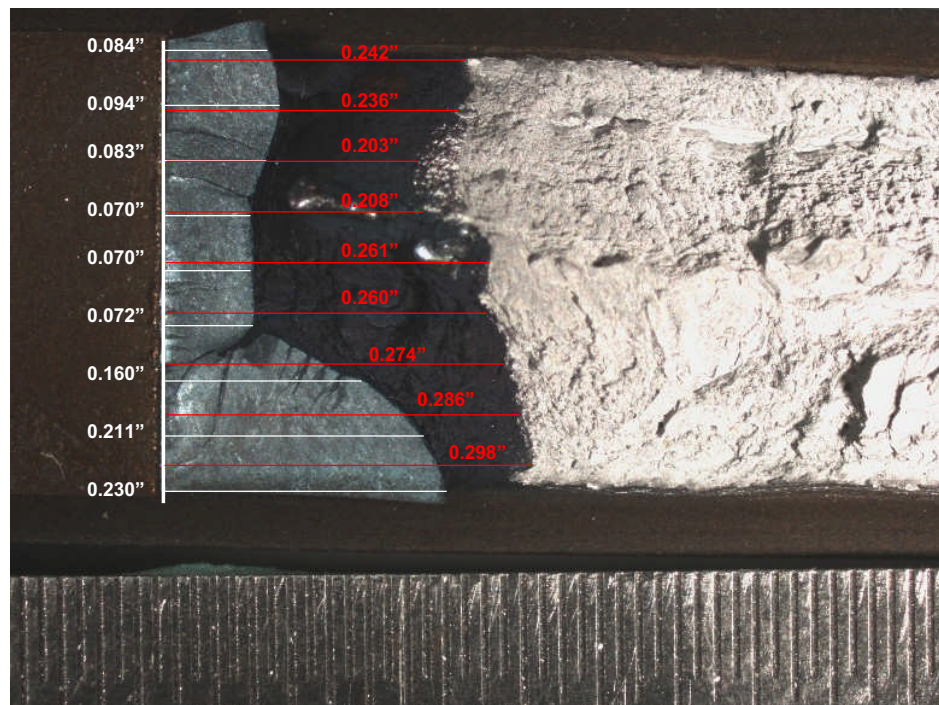


Figure A-6. Crack length measurements for specimen C2 (weld) of the flux-cored welded A516 steel

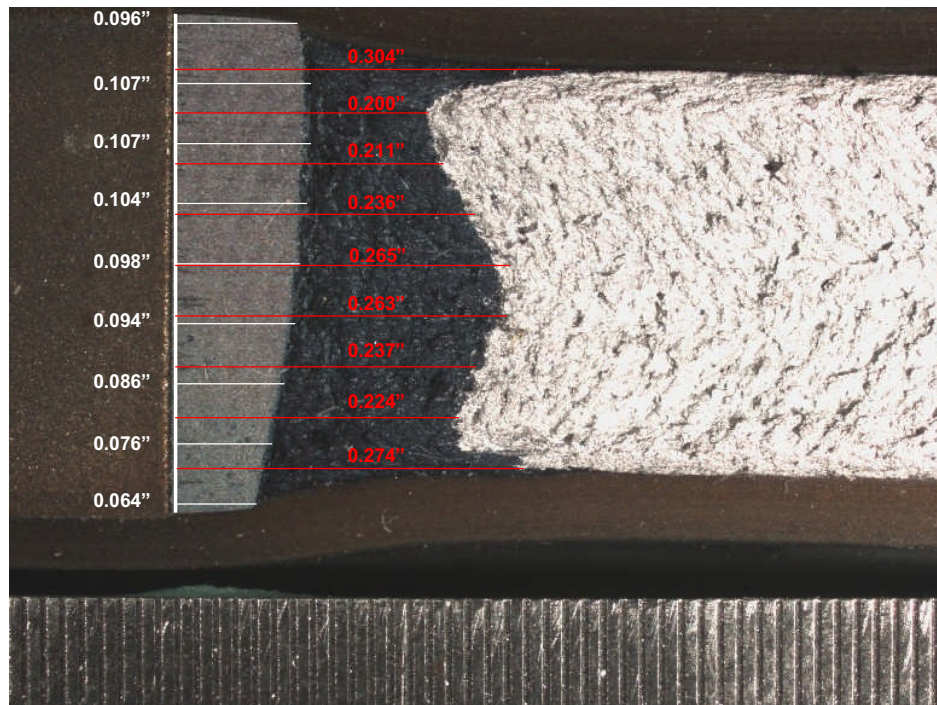


Figure A-7. Crack length measurements for specimen A2 (parent 0°) of the A516 steel

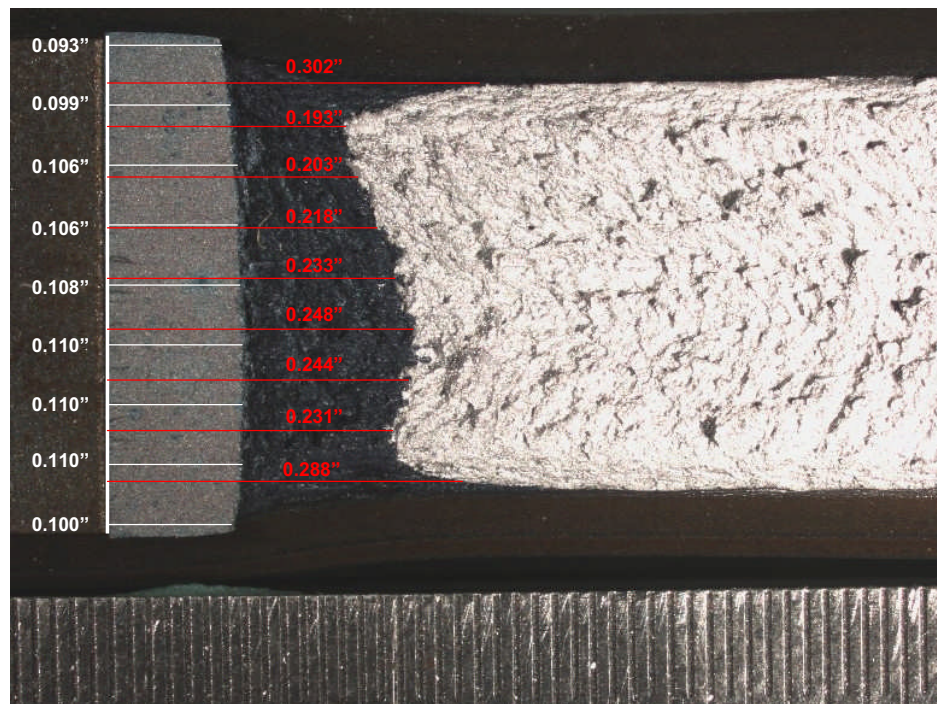


Figure A-8. Crack length measurements for specimen B3 (parent 0°) of the A516 steel

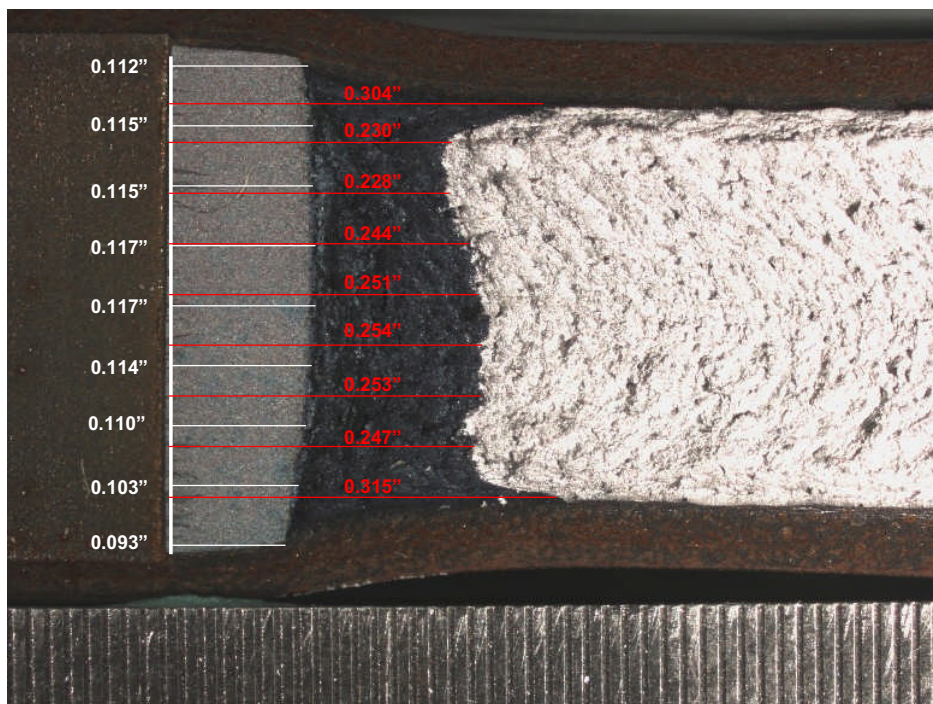


Figure A-9. Crack length measurements for specimen C3 (parent 0°) of the A516 steel



Figure A-10. Crack length measurements for specimen A4 (parent 90°) of the A516 steel

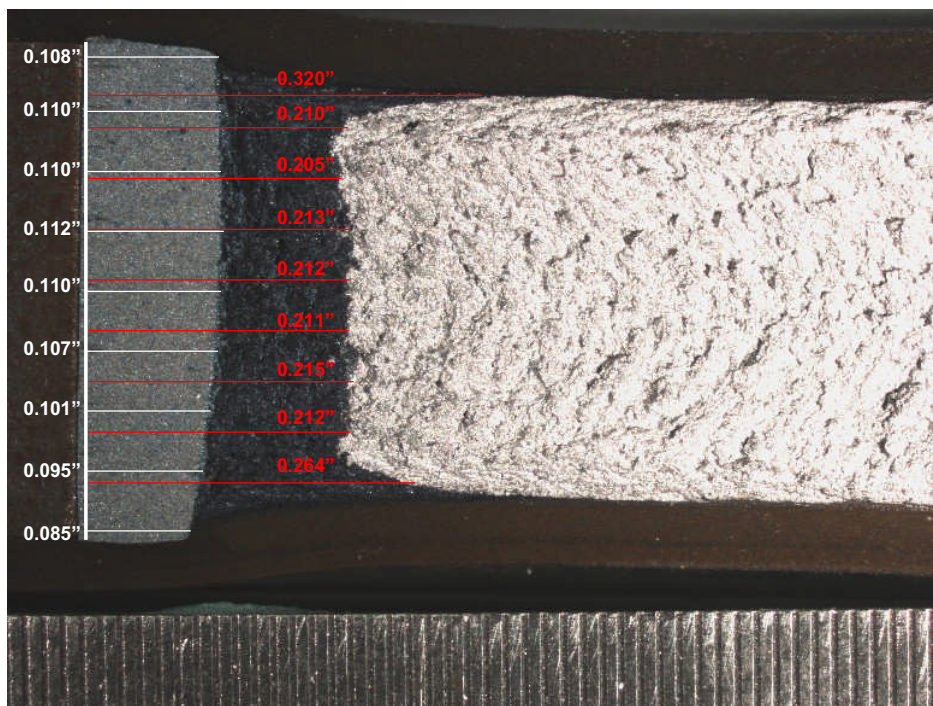


Figure A-11. Crack length measurements for specimen B4 (parent 90°) of the A516 steel

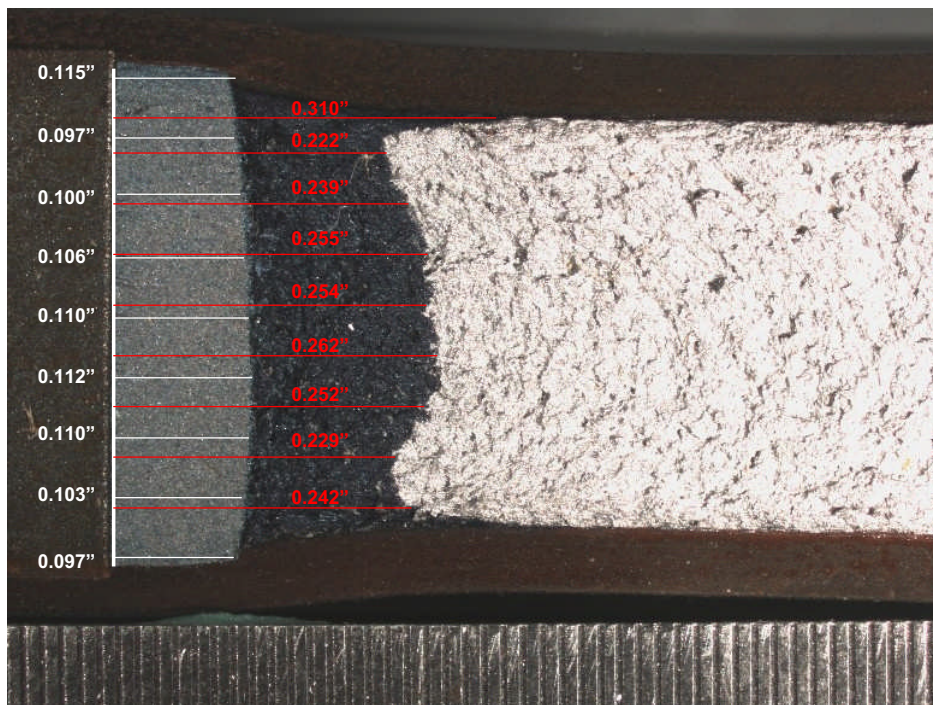


Figure A-12. Crack length measurements for specimen C4 (parent 90°) of the A516 steel

REPORT DOCUMENTATION PAGE

Form Approved
OMB No. 0704-0188

The public reporting burden for this collection of information is estimated to average 1 hour per response, including the time for reviewing instructions, searching existing data sources, gathering and maintaining the data needed, and completing and reviewing the collection of information. Send comments regarding this burden estimate or any other aspect of this collection of information, including suggestions for reducing this burden, to Department of Defense, Washington Headquarters Services, Directorate for Information Operations and Reports (0704-0188), 1215 Jefferson Davis Highway, Suite 1204, Arlington, VA 22202-4302. Respondents should be aware that notwithstanding any other provision of law, no person shall be subject to any penalty for failing to comply with a collection of information if it does not display a currently valid OMB control number.

PLEASE DO NOT RETURN YOUR FORM TO THE ABOVE ADDRESS.

1. REPORT DATE (DD-MM-YYYY) 01-08-2008			2. REPORT TYPE Technical Memorandum		3. DATES COVERED (From - To) December 2006 - January 2008	
4. TITLE AND SUBTITLE Ares I-X USS Material Testing			5a. CONTRACT NUMBER 510505.03.07.01.11 5b. GRANT NUMBER 5c. PROGRAM ELEMENT NUMBER 			
6. AUTHOR(S) Dawicke, David, S.; Smith, Stephen W.; and Raju, Ivatury S.			5d. PROJECT NUMBER 5e. TASK NUMBER 5f. WORK UNIT NUMBER 			
7. PERFORMING ORGANIZATION NAME(S) AND ADDRESS(ES) NASA Engineering and Safety Center Langley Research Center Hampton, VA 23681-2199				8. PERFORMING ORGANIZATION REPORT NUMBER L-19517 NESC-RP-08-09/06-081-E		
9. SPONSORING/MONITORING AGENCY NAME(S) AND ADDRESS(ES) National Aeronautics and Space Administration Washington, DC 20546-0001				10. SPONSORING/MONITOR'S ACRONYM(S) NASA 11. SPONSORING/MONITORING REPORT NUMBER NASA/TM-2008-215338		
12. DISTRIBUTION/AVAILABILITY STATEMENT Unclassified - Unlimited Subject Category 39 - Structural Mechanics Availability: NASA CASI (301) 621-0390						
13. SUPPLEMENTARY NOTES						
14. ABSTRACT An independent assessment was conducted to determine the critical initial flaw size (CIFS) for the flange-to-skin weld in the Ares I-X Upper Stage Simulator (USS). Material characterization tests were conducted to quantify the material behavior for use in the CIFS analyses. Fatigue crack growth rate, Charpy impact, and fracture tests were conducted on the parent and welded A516 Grade 70 steel. The crack growth rate tests confirmed that the material behaved in agreement with literature data and that a salt water environment would not significantly degrade the fatigue resistance. The Charpy impact tests confirmed that the fracture resistance of the material did not have a significant reduction for the expected operational temperatures of the vehicle.						
15. SUBJECT TERMS NESC, CIFS, Ares I-X USS, flange-to-skin weld						
16. SECURITY CLASSIFICATION OF:			17. LIMITATION OF ABSTRACT	18. NUMBER OF PAGES	19a. NAME OF RESPONSIBLE PERSON STI Help Desk (email: help@sti.nasa.gov) 19b. TELEPHONE NUMBER (Include area code) (301) 621-0390	
a. REPORT UU	b. ABSTRACT UU	c. THIS PAGE UU	UU	38		